Water Research 186 (2020) 116387

Contents lists available at ScienceDirect

Water Research

journal homepage: www.elsevier.com/locate/watres

Enhancing solar disinfection (SODIS) with the photo-Fenton or the Fe^{2+}/peroxymonosulfate-activation process in large-scale plastic bottles leads to toxicologically safe drinking water

Paloma Ozores Diez[a], Stefanos Giannakis[b,*], Jorge Rodríguez-Chueca[c,d], Da Wang[c,e], Bríd Quilty[a], Rosaleen Devery[a,*], Kevin McGuigan[f], Cesar Pulgarin[c]

[a] School of Biotechnology, Dublin City University (DCU), Glasnevin, Dublin 9, Ireland
[b] Universidad Politécnica de Madrid (UPM), E.T.S. Ingenieros de Caminos, Canales y Puertos, Departamento de Ingeniería Civil, Hidráulica, Energía y Medio Ambiente, Unidad docente Ingeniería Sanitaria, c/ Profesor Aranguren, s/n, Madrid, ES-28040, Spain
[c] School of Basic Sciences (SB), Institute of Chemical Science and Engineering (ISIC), Group of Advanced Oxidation Processes (GPAO), École Polytechnique Fédérale de Lausanne (EPFL), Station 6, Lausanne, CH-1015, Switzerland
[d] Universidad Politécnica de Madrid (UPM), E.T.S. de Ingenieros Industriales, Departamento de Ingeniería Química Industrial y del Medio Ambiente, c/ de José Gutiérrez Abascal 2, Madrid, 28006, Spain
[e] College of Environment, Zhejiang University of Technology, Hangzhou, 310032, China
[f] Department of Physiology & Medical Physics, Royal College of Surgeons in Ireland (RCSI), Dublin 2, Ireland

ARTICLE INFO

Article history:
Received 28 July 2020
Revised 1 September 2020
Accepted 2 September 2020
Available online 3 September 2020

Keywords:
Solar disinfection (SODIS)
Drinking water
Oxidation process
Toxicity
Plastic leachables
E. coli

ABSTRACT

Solar disinfection (SODIS) in 2-L bottles is a well-established drinking water treatment technique, suitable for rural, peri–urban, or isolated communities in tropical or sub-tropical climates. In this work, we assess the enlargement of the treatment volume by using cheap, large scale plastic vessels. The bactericidal performance of SODIS and two solar-Fe^{2+} based enhancements, namely photo-Fenton (light/H_2O_2/Fe^{2+}) and peroxymonosulfate activation (light/PMS/Fe^{2+}) were assessed in 19-L polycarbonate (PC) and 25-L polyethylene terephthalate (PET) bottles, in ultrapure and real water matrices (tap water, lake Geneva water). Although SODIS always reached total (5-logU) inactivation, under solar light, enhancement by or both Fe^{2+}/H_2O_2 or Fe^{2+}/PMS was always beneficial and led to an increase in bacterial elimination kinetics, as high as 2-fold in PC and PET bottles with tap water for light/H_2O_2/Fe^{2+}, and 8-fold in PET bottles with Lake Geneva water. The toxicological safety of the enhancements and their effects on the plastic container materials was assessed using the E-screen assay and the Ames test, after 1-day or 1-week exposure to SODIS, photo-Fenton and persulfate activation. Although the production of estrogenic compounds was observed, we report that no treatment method, duration of exposure or material resulted in estrogenicity risk for humans, and similarly, no mutagenicity risk was measured. In summary, we suggest that SODIS enhancement by either $HO^{\bullet}$- or $SO_4^{\bullet-}$-based advanced oxidation process is a suitable enhancement of bacterial inactivation in large scale plastic bottles, without any associated toxicity risks.

1. Introduction

Solar Disinfection (SODIS) is a World Health Organization (WHO)-approved intervention for the generation of safe drinking water prior to consumption. Its success is based on its simplicity in which a transparent container is filled with the available water and exposed to sunlight for one day (under normal irradiation conditions) or two days under cloudy skies (McGuigan et al., 2012). After this time, the microbial load, and especially bacterial counts, are significantly lower and the water is safer to drink. The interventions that have been successfully implemented all verified the acceptance of this method from the local population due to its simplicity, since only a water container (usually a 2-L polyethylene terephthalate (PET) bottle provided to the population participating in the actions), heat and sunlight are involved.

Despite its easy protocol, there are several pitfalls in the application that have instigated research over the past 30 years since the first guidelines were published (Wegelin et al., 1994). For instance, solar light is comprised of UVC light (which does not reach the Earth's crust), UVB, UVA, visible and infrared light (IR). Some

* Corresponding authors.
E-mail address: stefanos.giannakis@upm.es (S. Giannakis).

https://doi.org/10.1016/j.watres.2020.116387

materials used for SODIS vessels (e.g. polycarbonate or PET) are partially or completely opaque to UVB (Wegelin et al., 2001), UVA is significantly less energetic than UVB (Sinton et al., 1999), visible light is abundant but almost harmless to microorganisms and IR heats up water. The corresponding mode of action of each of the wavelengths has been recently reviewed (Giannakis et al., 2016; Nelson et al., 2018). Briefly, the main actions are: UVB light acts directly on the microorganism genome mutating its genetic material (Oppezzo, 2012; Pfeifer et al., 2005), UVA initiates oxidative chain reactions into the cell (in bacteria) (Berney et al., 2006; Bosshard et al., 2010a, 2010b; Giannakis, 2018; Hoerter et al., 2005) or matrix-related oxidative processes (Rosado-Lausell et al., 2013; Vione et al., 2010, 2006), visible light in the received intensities does not contribute much (Hessling et al., 2017; Ng et al., 2016) although recent reports indicate blue light-mediated bacterial inactivation (Halstead et al., 2019; Maclean et al., 2014), and the heat from IR light denatures proteins causing lethal damage (Baatout et al., 2005; Blaustein et al., 2013).

From the above description of the mode of action of SODIS and its applications, some obvious problems arise, which researchers have attempted to resolve over the past 30 years. For instance, PET filters out UVB, hence the efficacy of the process is reduced; consequently UVB-transparent materials, such as Pyrex bottles or polycarbonate vessels have been studied (Castro-Alférez et al., 2018; Fisher et al., 2012a; Keogh et al., 2015). UVB on the other hand mainly damages the genome, which means that the cell may still retain a capacity to repair its damage (via dark or light-assisted processes) and re-populate the water (Giannakis et al., 2014a; Vélez-Colmenares et al., 2012); hence oxidative processes have been proposed as improvements to the SODIS process (Byrne et al., 2015; Ndounla and Pulgarin, 2014; Polo-López et al., 2018). Among these processes, photo-Fenton (Spuhler et al., 2010) and more recently, persulfate activation (Guerra-Rodríguez et al., 2018) seem to be SODIS-compatible, since they exploit the majority of the solar spectrum (Huang et al., 2018; Mosteo et al., 2020; Rodríguez-Chueca et al., 2017), their reactants (Fe^{2+}, H_2O_2) are benign, part of the natural photochemical cycle (Voelker et al., 1997) or they leave harmless residual compounds (SO_4^{2-} in the case of persulfate) (Matzek and Carter, 2016). The efficacy of these processes has been documented in field tests; the generated oxidative species such as the $HO^{\bullet}$ and $SO_4^{\bullet-}$ inactivate cells by intracellular and/or extracellular disruption of their structural integrity and vital functions (Castro-Alférez et al., 2016; Ferreira et al., 2020; Giannakis et al., 2018; Xiao et al., 2020). Hence, they have proven regrowth elimination capacity (Moncayo-Lasso et al., 2009; Ndounla et al., 2013; Rincón and Pulgarin, 2007), and since they utilize relatively cheap reagents, many successful lab scale tests have been described in the literature.

Another issue highlighted frequently in feedback from communities using SODIS is that it is a labor-intensive process and the low batch volume of the bottles commonly used, i.e. 2-L PET, is not well-suited to family requirements. Since the early 2000's there have been many studies focusing on enlarging the treated volumes by solar collector reactors of higher capacity e.g. 20–25 L, up to 32–54 L and 88–140 L (Bichai et al., 2012; Martínez-García et al., 2020; Nalwanga et al., 2014; Polo-López et al., 2011; Reyneke et al., 2020; Ubomba-Jaswa et al., 2010), and larger than the standard PET plastic bottles, such as 19-L polycarbonate bottles and 5 or 20-L polypropylene buckets (Keogh et al., 2015; Polo-López et al., 2019). The apparent problems that were quickly addressed in the engineered systems (CPCs) were the increase of the optical path which is not beneficial for light transmission and the lower water temperatures generated in larger volumes. The latter has been proven a crucial parameter in the absence of light, but in abundant illumination it has a complementary synergistic character (Castro-Alférez et al., 2017; Giannakis et al., 2014b; McGuigan et al., 1998). Concerning the larger vessels, a vast series of materials (PVC, PMMA, PET, PC, and others) has recently been investigated on their light transmittance (García-Gil et al., 2020a). More specifically, aspects such as the wall thickness and wavelength-dependent light extinction have been examined because they ultimately affect the time required for total inactivation of bacteria.

Exposing water in plastic reactors to intense conditions of heat and light raises questions regarding the formation of photoproducts and the migration of compounds, from the containers into the water, which might be harmful to the consumer. Food contact materials are regulated by European Regulation No.1935/2004 (European Commission, 2004) which states that material in contact with food, which also includes drinking water, should not transfer its constituents to the food in quantities that could incur a risk to human health. The more recent European Regulation No. 10/2011 (European Commission, 2011) specifically covers plastic food-contact materials (FCM) and lists the compounds authorized for use in their manufacture. However, while intentionally added substances in plastics may be safe for the consumer, non-intentionally added substances (NIAS) in the final plastic material can be toxic to the consumer (Bach et al., 2013). In vitro bioassays, such as the Ames test and the E-screen assay, offer robust and economic solutions to screen for toxicity of FCM (Groh and Muncke, 2017). A limited number of toxicity studies have been carried out on the SODIS process. The Ames test has been used to test PET bottled water in SODIS-like conditions (De Fusco et al., 1990; Monarca et al., 1994; Ubomba-Jaswa et al., 2010), however, there are no reports of toxicity testing for advanced oxidative processes. Furthermore, studies to date have focused on PET plastic and so it was of interest to investigate toxicity associated with the advanced oxidative processes photo-Fenton and persulfate activation using PET and other plastics.

The present study aims to fill the knowledge gap concerning the suitability of large-volume plastic containers as SODIS or solar-assisted AOPs reactors and the safety of these materials in this regard. For this purpose, we have assessed two large-volume vessels for their suitability as SODIS and solar-assisted oxidative processes reactors for water treatment in the field. More specifically, a standard blue-tinted 19-L polycarbonate (PC) water dispenser bottle and a 25-L polyethylene terephthalate (PET) jerrycan have been subjected to conditions of solar disinfection (SODIS: no additives), solar light/H_2O_2, photo-Fenton (solar light/H_2O_2/Fe^{2+}), solar light/peroxymonosulfate (PMS) and (double) PMS activation (solar light/PMS/Fe^{2+}). The level of *E. coli* inactivation during these processes was monitored and the differences when distilled water (control), tap water and Lake Geneva water were used as experimentation matrix are reported. Finally, the suitability of the materials was studied by assessing the toxicity of the migrating compounds. The estrogenic and mutagenic effects of SODIS, $HO^{\bullet}$-based and $SO_4^{\bullet-}$-based AOPs was estimated after 1 or 7 days of consecutive tests.

2. Materials and methods

2.1. Chemicals and reagents

Iron (II) sulfate heptahydrate ($FeSO_4 \bullet 7H_2O$) ≥ 99%, peroxymonosulfate triple salt (PMS, Oxone™), potassium peroxydisulfate (PDS) and hydrogen peroxide (H_2O_2) 30%, were all provided by Sigma-Aldrich, Switzerland. The plate count agar and reagents for the preparation of the bacteriological media (NaCl, KCl, yeast extract) were also acquired from Sigma-Aldrich, Switzerland, while Bacto™ Tryptone was purchased from BD Biosciences, Switzerland. Beta-Estradiol (E2), ICI 182,780 (Fulvestrant) and cell culture media and supplements were purchased from Sigma-Aldrich, Ireland.

Table 1
Water matrices used in the study (own measurements and (Pulgarin et al., 2020; Shekoohiyan et al., 2019a, 2019b)).

Parameter	Units	Distilled water	Tap water	Lake Geneva water
Conductivity	μS/cm at 25 °C	<0.055	287	252
Transmittance at 254 nm	(%)	100	99.7	96
pH		6.25	8.15	8.3
Total organic carbon (TOC)	mg/L	<0.005	<0.005	0.9
Phosphate (PO_4^{3-})	mg/L		< 0.05	0.019
Bicarbonate (HCO_3^-)	mg/L		110	108
Chloride (Cl^-)	mg/L		11	8
Sulfate (SO_4^{2-})	mg/L		47	48
Nitrate (NO_3^-)	mg/L		3	2.7
Nitrite (NO_2^-)	mg/L		< 0.05	0.005
Total iron (Fe)	mg/L		0.092	0.01
Hardness	°f		13	13.6
Calcium (Ca^{2+})	mg/L		44	45.1
Magnesium (Mg^{2+})	mg/L		6	5.7
Sodium (Na^+)	mg/L		6.9	6.65
Potassium (K^+)	mg/L		1.8	1.7

2.2. Water matrices

In order to assess the differences and effects of water components on bacterial disinfection, the tests took place in distilled water (DI), tap water (without further pretreatment or chloride removal) and Lake Geneva water from the nearby pumping station of St. Sulpice, Lausanne, Switzerland. The main physicochemical characteristics of the water matrices are summarized in Table 1, obtained from own measurements and the Lausanne Water Services.

2.3. Bacterial preparation and enumeration methods

The *E. coli* K12 wildtype strain was originally obtained from the German Collection of Microorganisms and Cell Cultures (DSMZ, strain no. 498) and stored in 20% glycerol at −20 °C. The preparation method was previously published in detail (Giannakis et al., 2013; Marjanovic et al., 2018); briefly, one colony from a preculture was inoculated in 5 mL of sterilized Luria-Bertani (LB) broth (10 g/L Bacto™ Tryptone, 10 g/L NaCl and 5 g/L NaCl). The dispersion was incubated at 37 °C under shaking at 180 rpm for 8 h. Afterwards, 1% dilution was performed in LB and the solution was further incubated for 15 h under the same conditions. *E. coli* were separated from the medium by centrifuging at 5000 rpm for 15 min at 4 °C followed by a rinsing step with a sterile saline solution (8 g/L NaCl and 0.8 g/L KCl); the process was repeated three times, for 5 min, under the same conditions. The bacterial pellet was finally suspended in 25 mL of saline solution.

The concentration of the resulting bacterial stock was 10^9 Colony Forming Units per mL (CFU/mL). The initial concentration of 10^5 CFU/mL which was used throughout the disinfection experiments was obtained by dilution and was estimated by the standard plate count method on non-selective plate count agar (PCA). PCA plates were incubated for 24 h at 37 °C, followed by manual colony counting.

2.4. Plastics used in the study

Three types of plastic containers were used in the study – polyethylene terephthalate (PET) from a 25-L transparent container (which we used as jerrycan, PETjc), PET from a 500-mL coca cola bottle (PETcc) and blue polycarbonate (PC) from a 19-L container used in a water dispenser (see Table 2 for more information). Prior to the disinfection tests, the used Coca-Cola bottles were washed with ethanol, warm water with soap and rinsed multiple times with DI water. After the disinfection tests and prior to toxicity testing, the pieces of plastic were cleaned with 70% ethanol, rinsed with DI water, and cut into small pieces of $4 \times 4 mm^2$.

2.5. Experimental strategy of disinfection tests and toxicity assays

The objective of the study was to study the solar-assisted bacterial disinfection in large-volume reactors. The disinfection tests took place in the PET jerrycans and blue PC bottles. The disinfection capacity of solar light, photo-Fenton and solar/Fe^{2+} activated peroxymonosulfate were assessed in DI water (blank), tap water (real matrix in absence of organic matter) and Lake Geneva water (real water matrix with organic matter). Solar disinfection (no additives), solar light/H_2O_2, photo-Fenton (solar light/H_2O_2/Fe^{2+}), solar light/PMS and (double) PMS activation (solar light/PMS/Fe^{2+}) were assessed for their bactericidal efficacy. SODIS (hv) is considered the baseline process, the hv/H_2O_2 and photo-Fenton processes are the $HO^\bullet$-producing group of AOPs while hv/PMS and hv/PMS/Fe^{2+} are producing both $HO^\bullet$ and $SO_4^{\bullet-}$.

For the assessment of the toxicological safety of the plastic materials, a battery of tests was applied after disinfection. To achieve reproducible results in the most unfavorable conditions, the plastics were cut, and the migrating substances' toxicity was separately evaluated. To ensure a benchmark comparison with the new, food-approved PET jerrycan (PETjc), another already food-approved PET material was used (PET from Coca-Cola bottles, PETcc). The plastic bottles were cut in pieces and the respective amounts of material were submerged in 1 L of Milli-Q (MQ) water in a borosilicate glass vessel: PETjc (8.3 g), PETcc (15 g) and polycarbonate (PC, 14.5 g). The quantities of plastic used corresponded to the internal surface exposed for each original container, from which the plastic would leach into the water, divided by the quantity of water treated by the vessel. The use of MQ water prevented any interference from the water matrix and the use of borosilicate glass vessel any further leachables generation. For the toxicity tests, solar light, photo-Fenton and PDS activation (instead of PMS) by solar light and Fe^{2+} were assessed; PMS activation leads to hydroxyl and sulfate radicals' generation hence in order to dissociate the effects of $SO_4^{\bullet-}$, PDS was used as a precursor, to avoid simultaneous $HO^\bullet$ generation by the oxidant and have only the possibility of its partial generation from side reactions ($SO_4^{\bullet-}$ reaction with HO^-).

2.6. Solar-based treatment methods used in the study

The disinfection tests were carried out on the terrace of the Swiss Federal Polytechnic School, Chemistry building, under clear days in July and August (Lat: 46.5191° N, Long: 6.5668° E). The bottles were placed standing on their base, on a metallic surface (sub-optimal configuration for reflectance and effective irradiation surface area use) to simulate as unfavorable conditions as possible, on the assumption that any enhancements might be more readily

Table 2
Plastic bottles used in the study and their geometrical characteristics.

Pictures (right) and characteristics of the used bottles (below)		
Measurements	**PC bottle**	**PET jerrycan**
Volume (L)	19	25
Height (cm)	48	53
Diameter (cm)	27	-
Length (cm)	-	28
Width (cm)	-	24
Optical path (cm)	13.5	12
Thickness (mm)	1.4	0.55

observed; see Fig. S1 for the setup configuration. The global solar irradiance was monitored using a Kipp & Zonen (CM3) pyranometer and the values were recorded automatically in 1-min intervals, from which the total solar energy was calculated, while temperature was recorded manually. The selected concentrations were Fe^{2+}: 1 ppm (18 μM), H_2O_2: 10 ppm (290 μM) for the solar/H_2O_2 and the photo-Fenton processes, while Fe^{2+}: 1 ppm (18 μM) and 2.74 mg/L Oxone^{TM} (36 μM) were used for the solar and solar/Fe^{2+} activation of PMS. Kinetic analysis was performed in Origin Software, by fitting log-linear curves.

For the toxicity tests, solar irradiation was simulated by a SUNTEST Solar Simulator, using a 1500 W Xe lamp, with a wavelength spectral distribution of approx. 0.5% of emitted photons <320 nm (UV-B range) and about 5–7% between 300 and 400 nm (UVA range). The emission spectrum between 400 and 800 nm follows the solar spectrum. Light intensity was set at 1000 W/m^2 and was pre-calibrated with a Kipp & Zonen (CM3) pyranometer. The irradiation experiments were started at room temperature (25 °C) and the temperature of the solution increased up to approximately 30 °C during irradiation, due to the air-cooling system of the SUNTEST. All experiments were carried out in equilibrium with air agitation at 700 rpm.

Three different treatments were used. Solar disinfection (SODIS) without any enhancements, photo-Fenton (solar light/H_2O_2/Fe^{2+}) using 10 ppm (290 μM) H_2O_2 (Riedel-de Haën, Germany) and 1 ppm (18 μM) Fe^{2+} and persulfate activation (solar light/PDS/Fe^{2+}) using 24.3 ppm (90 µM) peroxydisulfate (PDS) and 1 ppm (18 μM) Fe^{2+}; the values were selected for their expected efficacy according to previous studies (Marjanovic et al., 2018; Rodríguez-Chueca et al., 2019).

Two time periods of irradiation were investigated – 6 consecutive hours for 1 day, and 6 consecutive hours a day for 7 consecutive days (1 week). Corresponding control vessels were incubated in the dark. Following incubation, water samples were extracted using solid phase extraction and analyzed for estrogenicity using the E-screen method and for mutagenicity using the Ames test.

2.7. Solid Phase Extraction (SPE) of the treated water samples

Water samples were extracted using a modification of the solid phase extraction method described by Wagner and Oehlmann, and Abbas et al. (Abbas et al., 2019; Wagner and Oehlmann, 2011). Oasis HLB Glass Cartridges (5cc/200 mg LP by Waters Chromatography, Ireland Ltd) were conditioned by pouring 4 ml acetone into the cartridge. The acetone was collected, discarded and the step was repeated. The cartridge was then equilibrated by pouring 4 mL distilled water. The water was collected, discarded and the procedure was repeated. The cartridges were set up on a Waters 20 position extraction manifold (Waters Corporation, Milford, MA, USA) connected to a Waters vacuum pump (220 V, 50 Hz). The treated water sample by a solar-assisted process (1 L) was loaded onto the cartridge and extracted under vacuum using a flow rate of 12 mL/min. The effluent was then collected and discarded. The dry cartridge was eluted with 4 mL HPLC grade methanol which was

collected in a 7 mL capacity glass vial (Fisherbrand™ Bijou Type III soda lime) with a polypropylene cap. DMSO (100 µL) was added into the vial. The methanol was removed under a gentle stream of nitrogen yielding final extracts in 100 µL DMSO (concentration factor: x10.000). The glass vial with PP cap was stored at −20 °C until analyzed. To assess recovery of estrogenic compounds water was spiked with a range of concentrations (10^{-14} M to 10^{-6} M) of the synthetic xenoestrogen BPA or endogenous estrogen E2. Recovery was determined by comparing proliferative effects of spiked water extracts with effects of equivalent concentrations of BPA and E2 (10^{-14} M to 10^{-6} M) that did not undergo extraction. Average% recovery was 93%.

2.8. E-screen bioassay

Endocrine disruption is the potential consequence of exposure to chemicals that may interfere with the endocrine system. The E-screen is a mammalian assay estrogen screen that measures (xeno) estrogen-induced cell proliferation in MCF-7 cells. Prior to the E-screen, the solid phase extracted samples (in DMSO) were diluted 100-fold with cell culture medium resulting in a final solvent negative control concentration of 1% (v/v). The cell culture conditions for the E screen, described by Soto et al. (Soto et al., 1995), were used with minor modifications and cell number was quantified based on DNA binding to the fluorescent Hoechst 33,258 dye as described by Papadimitriou and Lelkes (Papadimitriou and Lelkes, 1993).

Briefly, MCF-7 BOS cells (kindly donated by Professor Ana M Soto, Tufts University School of Medicine Boston, MA) were routinely maintained in DMEM medium with phenol red and supplemented with 5% fetal bovine serum. Prior to treatment, the cells were seeded on 96 well plates at an initial density of 4000 cells/well. After 24 h to allow cell attachment, the cell culture medium was replaced with 100 μL medium containing controls (medium alone (blank), 1% (v/v) DMSO in medium (negative), medium containing 1 nM E2 (positive)), 100-fold diluted sample extracts (final concentration factor 100 X) and 100-fold diluted sample extracts with ICI 182,780 (1 μM), an estrogen antagonist. Hormone-free cell culture medium (DMEM/F12 without phenol red) containing 2.5% newborn calf serum and 2.5% charcoal stripped fetal bovine serum and 2 mM glutamine was used during the assay and for sample dilutions. The proliferative response of the E screen bioassay was validated using 17-β estradiol (0.01 pM-1 μM). After 6 days of incubation at 37 °C in 5% CO_2 proliferation was determined using the fluorescence dye Hoechst 33,258.

2.9. Data interpretation and analysis

Fluorescence emission of each water extract was normalized to fluorescence emission of the negative control giving the proliferative effect (PE) of the water extract (Equation 1: Calculation of Proliferative Effect).

$$\mathrm{PE} = \frac{\text{Water extract fluorescence}}{\text{Negative Control fluorescence}} \times 100 \quad (1)$$

The estrogenic activity of the water extracts was evaluated by determining relative proliferative effect (RPE). The RPE (% E2) compares the maximal fluorescence produced by the water extract with the fluorescence emitted by the positive control (1 nM E2) (Equation 2: calculation of Relative proliferative effect index,% E2).

$$\mathrm{RPE} = \frac{\text{Water extract fluorescence} - \text{Negative Control fluorescence}}{\text{E2 fluorescence} - \text{Negative Control fluorescence}} \times 100 \quad (2)$$

Total agonists of E2 were defined by Kuch et al. (Kuch et al., 2010) as samples having RPE between 80% and 100% relative proliferation. Partial agonists were defined as samples having RPE between 25% and 80% relative proliferation while weak agonists were defined as samples having RPE between 10% and 25% respectively. Finally, non-estrogenic substances will have RPE values between 0 and 10%. Estradiol equivalents (EEQ) were calculated by interpolation from a dose response curve of 17 β estradiol in the range 0.01 pM to 1 nM E2 (data not shown) (Equation 3: Equation for the interpolation of EEQ values from the dose response curve of 17 β estradiol).

$$y = 8500.6x^{0.2096} \quad (3)$$

EEQ were corrected for final concentration factor and reported as ng/L of the original water sample. Three independent experiments were conducted on each sample.

Graphs were plotted as the mean ± SD of the PE using the Excel Microsoft office software. Data analysis was performed using IBM SPSS statistics 25, all the data points that fell more than 1.5 times the interquartile range above the third quartile or below the first quartile (1.5IQR) were consider outliers and removed. Analysis of variance (single factor ANOVA) was used to compare the effects of the different treatments on the MCF-7 proliferative effect; followed by a Tukey and Game-Howell Post Hoc analysis. All differences were considered statistically significant when $p<0.05$.

2.10. The Ames test

In order to assess the genotoxic/mutagenic activity of the water samples, the Ames test was employed; genotoxicity refers to the ability of toxic agents to damage the genetic material in the cells. Samples for testing were first extracted using the SPE method described above. The samples were concentrated 1000-fold and 10μL volumes were tested for mutagenicity/genotoxicity using the Ames II kit by Xenometrix AG (Allschwil, Switzerland). The kit contains *S. typhimurium* strains TA98 used for the detection of frameshift mutations and TAMix a mixture of equal proportions of the Ames II TA7001-TA7006 strains to detect base-pair substitutions. Freshly prepared overnight cultures of TA98 and TAMix were exposed to the test sample as well as to a positive and negative control for 90 min in exposure medium containing sufficient histidine to support a few cell divisions. After 90 min exposure, cultures were diluted in pH indicator medium lacking histidine and aliquoted into 48 wells of a 384-well plate. Within 2 days, cells that had undergone the reversion to histidine prototrophy—either spontaneously, or, as a result of the exposure to a mutagen— grew into colonies. Bacterial metabolism reduces the pH of the medium, changing the color of that well from purple to yellow. The number of wells containing revertant colonies was counted for each sample and compared to a solvent (negative) control. The result was expressed as the fold increase over the baseline which was the ratio of the mean number of positive wells for the dose concentration divided by the baseline. The baseline was obtained by adding one standard deviation to the mean number of positive wells of the solvent control. A sample that showed a clear fold induction ≥2 above the baseline was classified as a mutagen. The mutagenic potential of the samples was assessed directly and in the presence of liver S9.

3. Results and discussion

3.1. E. coli *disinfection tests in PC and PET bottles, under SODIS and oxidative methods*

Figs. 1-4 summarize the disinfection experiments that took place in the two large-scale bottles, namely the 19-L blue polycarbonate bottle and the 25-L polyethylene terephthalate jerrycan

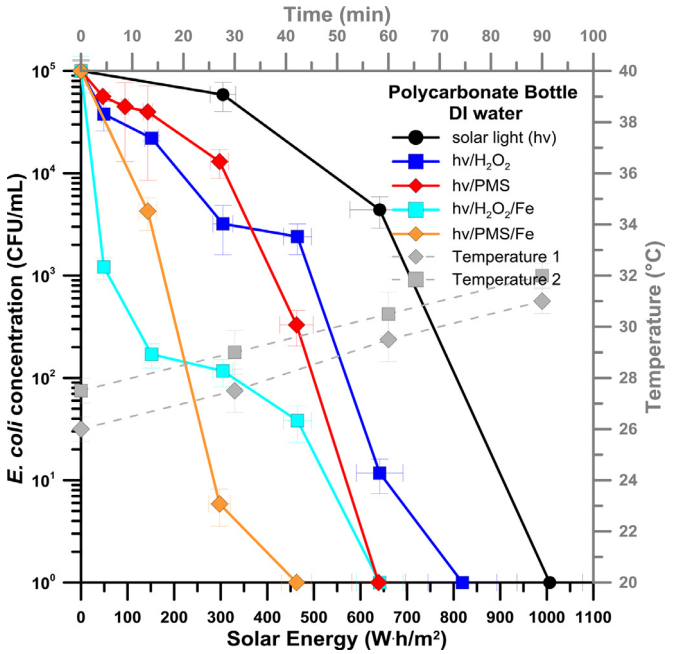

Fig. 1. Solar disinfection and enhancement experiments (hv/H_2O_2, $hv/H_2O_2/Fe^{2+}$, hv/PMS and $hv/PMS/Fe^{2+}$) in the Polycarbonate bottle, with distilled water. Initial concentrations of added reagents: $[Fe^{2+}]_0$ = 18 μM, $[H_2O_2]_0$ = 290 μM, $[PMS]_0$ = 36 μM. The vertical bars indicate the standard deviation from the mean bacterial concentration while the horizontal ones the SD of the received solar energy. Temperatures 1 and 2 (square and diamond traces) refer to the climatological conditions of the days when PMS or H_2O_2 based experiments took place, respectively (SODIS was always performed as control).

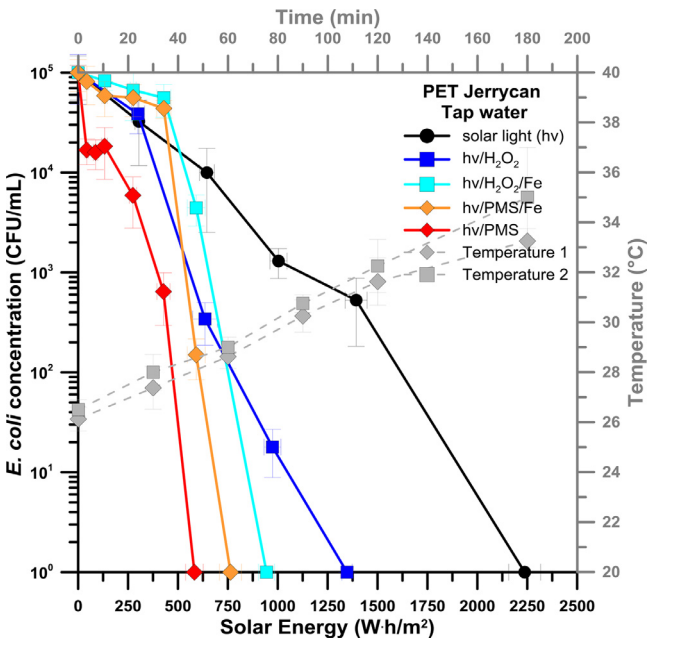

Fig. 3. Solar disinfection and enhancement experiments (hv/H_2O_2, $hv/H_2O_2/Fe^{2+}$, hv/PMS and $hv/PMS/Fe^{2+}$) in the PET jerrycan, with tap water. Initial concentrations of added reagents: $[Fe^{2+}]_0$ = 18 μM, $[H_2O_2]_0$ = 290 μM, $[PMS]_0$ = 36 μM. The vertical bars indicate the standard deviation from the mean bacterial concentration while the horizontal ones the SD of the received solar energy. Temperatures 1 and 2 (square and diamond traces) refer to the climatological conditions of the days when PMS or H_2O_2 based experiments took place, respectively (SODIS was always performed as control).

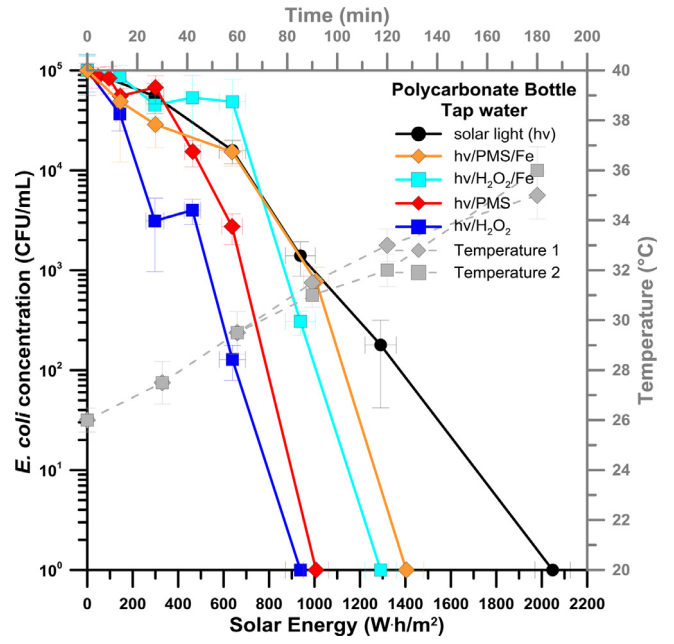

Fig. 2. Solar disinfection and enhancement experiments (hv/H_2O_2, $hv/H_2O_2/Fe^{2+}$, hv/PMS and $hv/PMS/Fe^{2+}$) in the Polycarbonate bottle, with tap water. Initial concentrations of added reagents: $[Fe^{2+}]_0$ = 18 μM, $[H_2O_2]_0$ = 290 μM, $[PMS]_0$ = 36 μM. The vertical bars indicate the standard deviation from the mean bacterial concentration while the horizontal ones the SD of the received solar energy. Temperatures 1 and 2 (square and diamond traces) refer to the climatological conditions of the days when PMS or H_2O_2 based experiments took place, respectively (SODIS was always performed as control).

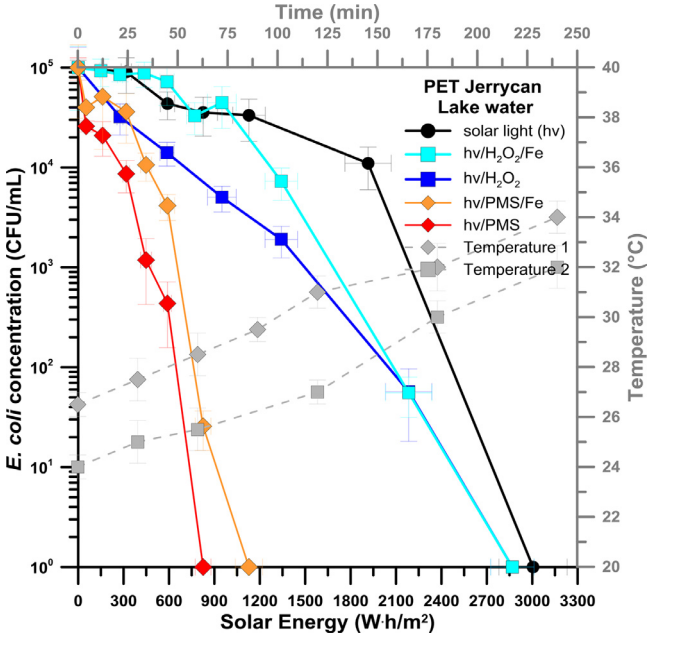

Fig. 4. Solar disinfection and enhancement experiments (hv/H_2O_2, $hv/H_2O_2/Fe^{2+}$, hv/PMS and $hv/PMS/Fe^{2+}$) in the PET jerrycan, with Lake Geneva water. Initial concentrations of added reagents: $[Fe^{2+}]_0$ = 18 μM, $[H_2O_2]_0$ = 290 μM, $[PMS]_0$ = 36 μM. The vertical bars indicate the standard deviation from the mean bacterial concentration while the horizontal ones the SD of the received solar energy. Temperatures 1 and 2 (square and diamond traces) refer to the climatological conditions of the days when PMS or H_2O_2 based experiments took place, respectively (SODIS was always performed as control).

Table 3
Summary of the bacterial inactivation kinetics, grouped per material and per treatment process.

	PC MQ Water		PC Tap Water		PET Tap Water		PET Lake Water	
k (min^{-1})	Value	Std. Error	Value	Std. Error	Value	Std. Error	Value	Std. Error
SODIS (hv)	0.0984	0.0234	0.0471	0.0044	0.0442	0.0017	0.0114	0.0008
hv/H_2O_2	0.1242	0.0137	0.0983	0.0097	0.0910	0.0095	0.0377	0.0019
hv/H_2O_2/Fe^{2+}	0.2124	0.0438	0.0684	0.0133	0.0851	0.0218	0.0275	0.0051
hv/PMS	0.1047	0.0129	0.0470	0.0066	0.1114	0.0118	0.0929	0.0055
hv/PMS/Fe^{2+}	0.2723	0.0203	0.0466	0.0051	0.1062	0.0221	0.0727	0.0090

(hereon: PC and PET, respectively). Since the bacterial inactivation mechanisms of SODIS, hv/H_2O_2, hv/H_2O_2/Fe^{2+} (photo-Fenton), hv/PMS and hv/PMS/Fe^{2+} have been previously discussed in the Introduction section; interested readers should refer to: (S. Giannakis et al., 2016; Marjanovic et al., 2018; Rodríguez-Chueca et al., 2019; Xiao et al., 2019), here we will not extensively discuss the pathways to inactivation but will focus only on the main driving forces under the given conditions and the new propositions due to the changes in the container material and the water matrix in which the experiments took place.

3.1.1. 19-L PC bottle with DI water

Fig. 1 showcases the experiments that took place in PC bottle, in DI water. Solar disinfection (hv alone) attained total (5-logU) bacterial inactivation within a reasonable timeframe (90 min), given the moderate ambient temperatures. The kinetics resemble the typical log-linear inactivation after a lag period. Our results are in accordance with the ones of Keogh et al. (Keogh et al., 2015), where total inactivation of 6-log *E. coli* was attained in 2 h in Spain in similar reactors (same material, volume, color and thickness).

SODIS inactivates bacteria mainly via the solar light UV and visible wavelengths (optical pathways) and heat (thermal pathway). The temperature during experimentation never surpassed 32 °C which is not expected to inactivate bacteria; on the contrary it is close to the optimal temperature for the survival of the mesophilic *E. coli* (37 °C) (Giannakis et al., 2014b). Hence, inactivation is attributed solely to the light-mediated pathways. Similarly to Keogh et al. (Keogh et al., 2015), the PC reactor permits the transmittance of the UV part in the UVB region of 290–320 nm, which has significant germicidal capacity and the UVA region (320–400 nm), which initiates a lethal intracellular cascade of oxidation events in bacteria (transmittance of PC: see Fig. S2). However, the transmittance reaches a plateau around 55% for the visible light. Although visible light has limited effect in the direct *E. coli* inactivation its participation is crucial in the other processes (to be discussed at later stage).

Addition of H_2O_2 in the water bulk enhanced *E. coli* inactivation (+26%) because it initiates two parallel disinfection events: i) the extracellular oxidation and, ii) after the passage of H_2O_2 into the cell, the enhancement of the oxidative events initiated by UVB and UVA light. The simultaneous presence of H_2O_2 and Fe^{2+} induces the generation of hydroxyl radicals in the bulk and into the cell via the Fenton process, hence the observed enhancement of E. coli inactivation compared to SODIS (116%). Fe^{3+} precipitates in near-neutral pH hence, the photo-Fenton is driven by colloidal iron forms, iron oxides and water-bound ligands (Farinelli et al., 2020), which, considering the different kinetics of heterogeneous processes against the homogeneous ones explain the short delay shown.

The addition of PMS into the water bulk enhanced SODIS (47%), initiating the oxidation of *E. coli*, similarly to previous works (Rodríguez-Chueca et al., 2019, 2017). In the PC reactor, we attain an activation of the PMS to generate hydroxyl and sulfate radicals, via the homolysis of the O–O bond. Although only UVC light was believed to activate the peroxide bond, recently, UVB and UVA irradiation have shown to be able to activate PDS and H_2O_2 and initiate the generation of radicals (Huang et al., 2018); in fact, in PMS this process should be easier due to the asymmetric structure of the precursor molecule, when compared with PDS (Flanagan et al., 1984). Addition of Fe^{2+} will initiate another pathway, the metal-induced PMS activation with Fe^{2+} oxidation to Fe^{3+}. However, PMS has been proven to reduce Fe^{3+} to Fe^{2+}, allowing its further activation, with the simultaneous production of $SO_5^{\bullet-}$ radical which is considered to have germicidal capacities (Rodríguez-Chueca et al., 2019). Hence, the consecutive addition of PMS and PMS/Fe^{2+} under solar light induces an increase in the inactivation kinetics (177%). A summary of the kinetics from which the improvement% was calculated is presented in Table 3.

3.1.2. 19-L PC bottle with tap water

Fig. 2 summarizes the experiments that took place in the same reactor but in tap water instead of DI water. Firstly, similar temperature profiles between the days of experimentation in DI and tap water are reported, hence there are no differences in thermal induced effects, e.g. light-thermal synergy (Castro-Alférez et al., 2017; McGuigan et al., 1998) or PMS activation (Rodríguez-Chueca et al., 2019). Table 1 of the Materials and Methods details the differences among the two matrices, with the two most significant being the alkaline pH of tap water (8.15), the presence of ions and a small absorbance in the far UVB region. Under solar light, the pH does not significantly influence bacterial inactivation, but the presence of ions eases the osmotic pressure that *E. coli* suffer in their absence (in DI water). Also, some of the ions contained the water have a small light absorbance (Rommozzi et al., 2020), hence the little difference in the UV–vis absorption spectra between DI and tap water (Fig. S3); these two actions lead to a 50% decrease in disinfection kinetics in tap water.

The changes in pH and the presence of ions have a more significant influence in the radical-based processes. More specifically, all processes are hindered significantly by the changes in the matrix, except H_2O_2 (−13%); its main action mode (after diffusion into the cell) does not get highly affected. H_2O_2 is an uncharged compound and the change of the overall *E. coli* charge at the new pH (isoelectric point of *E. coli* < 4, likely ~2.5 (Hairden and Harris, 1953; Rijnaarts et al., 1995)) does not hinder its passing into the cell. However, the addition of Fe^{2+} and the induction of the photo-Fenton process is significantly affected (−68%). Although the photo-Fenton process eventually inactivates *E. coli* 45% faster than SODIS, we observe that the kinetics are slower than the absence of Fe^{2+}. As it can be seen in Figure S4, the addition of Fe^{2+} in tap water leads to a rapid oxidation and a yellow tint in water from the beginning of the experiment, hence, the slow, plateau-like performance of the photo-Fenton process. The delay of the process can be attributed to the light attenuation of the precipitated iron (García-Gil et al., 2020b). A similar problem was encountered in another study with the same tap water (Pulgarin et al., 2020) and the use of citrate was employed as an iron chelator to prevent its rapid precipitation. Also, scavenging of $HO^{\bullet}$ is expected; Cl^-, HCO_3^-

and NO_3^- react with $HO^\bullet$ to generate $Cl^\bullet$, $CO_3^{\bullet-}$ and $NO_3^\bullet$ radicals, which are less oxidative than $HO^\bullet$ (hence less germicidal) while sulfates scavenging does not lead to reactive radicals at this pH (Rommozzi et al., 2020).

The hv/PMS process is also affected by the change in pH (−66%). The reasons between this delay are most likely i) the difficulty to come in contact with *E. coli* and induce extracellular oxidation (*E. coli* are now more negative and HSO_5^- is an anion), ii) the ineffective reaction of PMS with water components (e.g. with Cl^- that generates less oxidative radicals) iii) and the shift from a $SO_4^{\bullet-}$ to a more $HO^\bullet$ dominated inactivation process (Liu et al., 2015), due to the high presence of -OH. All possibilities are corroborated by the higher reduction in the efficacy of hv/PMS than the respective hv/H_2O_2 process. Also, especially in the case where PMS is activated by Fe, the same optical reasons that delayed photo-Fenton also apply here, leading to an 83% kinetics reduction compared to the DI water experiments. Furthermore, the $SO_4^{\bullet-}$ generated is less scavenged by water matrix ions than $HO^\bullet$ (Wang et al., 2020) hence the hv/Fe^{2+} activation of PMS results in basic pH results in slower kinetics than the hv/PMS process. Despite the possibility of PMS to reduce Fe, the generation of $SO_5^{\bullet-}$ is also not the most effective way to inactivate *E. coli*.

We should note here that in terms of inactivation kinetics the H_2O_2-based processes enhanced SODIS more than the PMS ones, for the selected amounts of Fe, H_2O_2 and PMS. More specifically, the benefit of adding H_2O_2 or H_2O_2/Fe^{2+} in the SODIS process is 130 and 45% respectively, while for the PMS and PMS/Fe^{2+} additions, the increase in PC and tap water is negligible (8 and 5%). Hence, the H_2O_2-based processes seem to be better enhanced in PC bottles.

3.1.3. 25-L PET jerrycan with tap water

Fig. 3 details the experiments that took place in the 25-L PET jerrycan and the point of comparison is the plastics used in the reactor (i.e. we will not repeat the ion-related issues discussed in Fig. 2). The first difference is the slightly higher volume of the PET jerrycan (25 vs. 19 L), but the optical pathway of the two reactors is relatively close, so we do not consider it a key aspect (the bottles' differences were summarized in Table 2). Also, we can factor out any temperature influence due to the consistency of the weather during the days of experimentation.

The inactivation kinetics of SODIS alone were very similar in the two types of reactor; in the PET bottle almost the same dose was necessary to achieve 5-logU reduction of the bacterial load compared to the PC reactor (only 6% faster in PC). In our opinion, this fact is actually a coincidence, considering the big differences in the reactor color, thickness and consequently the transmission in the water bulk. Firstly, PC does allow some UVB to get transmitted into the water bulk, but PET effectively blocks all wavelengths below 320 nm (0.8% transmittance at 319 nm, 1.95% at 320 nm, see Fig. S2). Moreover, it has been recently calculated that the thickness and the material can greatly influence the outcome of the disinfection process (García-Gil et al., 2020a); between a PC bottle with 2 mm thickness and a PET one with 0.5, the PET shows more than 25% higher UV–vis transmittance. Our material is ~1.5 mm thick, but has a blue tint, so this range of reported difference is not far from our case. Hence, we have to consider a complete shift in the underlying inactivation mechanisms induced by light alone. In PC, UVB acts at DNA level and UVA induces the intracellular photo-Fenton process, but in PET bottles the former is not active at all. However, the UVA levels transmitted in the PET Jerrycan are significantly higher than the PC, and most likely compensate the loss of the highly energetic UVB photons by the ample transmittance of the UVA ones. These results cannot be scaled with the ones by Keogh et al. (Keogh et al., 2015), since a 2-L PET bottle was used there, but the transmittance of the Jerrycan is comparable with the standard SODIS bottle, if not a little higher (Fig. S2); hence the material is an excellent choice for SODIS, no worse than the PC tested before by Keogh et al. (Keogh et al., 2015).

The transparent color of the PET jerrycan and its smaller thickness allows significantly higher light transmittance in the PET reactor in the UVA-vis region. This fact affects the performance of some of the oxidative processes. More specifically, the hv/H_2O_2 process is mildly affected (4-logU instead of 5-logU reduction in 1000 Wh/m^2, −16%) due to this shift. The reason is that PET does not allow UVB transmittance, which still has a small capacity of homolytic disruption of H_2O_2 to generate $HO^\bullet$, hence the experiments in PET lose this pathway compared to PC due to the tenfold drop of the homolytic quantum yield between UVB and UVA (Zuo and Hoigne, 1992). Nevertheless, the much higher UVA-vis light transmitted, in presence of H_2O_2 allows the intracellular photo-Fenton to take place and compensate the loss of the extracellular pathway. Hence the overall efficacy remains the same. The photo-Fenton process itself is now not hampered (24% kinetics' increase), since the PET allows higher UVA transmittance that initiates the intracellular events, but also an important difference in visible light, which also affects *E. coli* (Mosteo et al., 2020) and assists in iron recycling, increasing the small extent that it takes place (intracellular events, LMCT in the bacterial cell wall) (Giannakis et al., 2018).

The hv/PMS process is highly benefited from the change in material (118% increase in kinetics). As a matter of fact, almost half the energy is required to inactivate 5 logU of *E. coli*. The explanation behind this change lies within the photo-activity of PMS in the UV–vis range. Fig. S5 depicts the molar absorption coefficient of H_2O_2 and PMS, where significantly higher values are observed for the latter. As such, we postulate that UVA (and vis light) can effectively activate PMS, being the only wavelengths that are transmitted in the reactor. Furthermore, although the PET does not permit UVB, the significantly higher UVA and visible light transmitted over-compensate its loss; UVA and visible light have been previously proved to synergistically inactivate *E. coli* (Rodríguez-Chueca et al., 2019) and is verified here as well. The addition of Fe^{2+}, similarly to the photo-Fenton process, although it reduces the efficacy of the hv/PMS process, the difference is now much lower with hv/PMS most likely due to the Fe^{3+}-PMS activity reported in literature; Fe^{3+} under UVA/vis has been found to enhance PMS-mediated degradation of contaminants (Hasan et al., 2020). Also, almost half the required energy is required for the total *E. coli* inactivation in the PET Jerrycan compared to the PC bottle (114% increase in kinetics). The iron-related mechanisms are functioning in a higher degree than the PC bottle hence the overall decrease in solar energy dose. Hence the PET, at these dimensions and thickness, despite the loss of the UVB photons is deemed a good alternative material for both SODIS and oxidative processes.

It is noteworthy that, for the selected amounts of Fe, H_2O_2 and PMS, the addition of H_2O_2 and H_2O_2/Fe^{2+} in the SODIS process resulted in 106 and 93% increase in tap water in the PET jerrycan, while 152 and 140% were the corresponding PMS and PMS/Fe^{2+} increases in kinetics (compared to SODIS). There is no doubt that the addition of, at least the oxidant, greatly impacts the inactivation kinetics. Also, compared with the levels of enhancement noted in the PC bottle reactor (130, 45, 8, 5%), the H_2O_2 ones performed similarly (slightly better) but the PMS processes effectiveness increased dramatically. As such, one may attribute H_2O_2 based enhancements in PC reactors which allow more UVB, while PMS-based enhancements should be preferred in PET reactors.

3.1.4. 25-L PET jerrycan with Lake Geneva water

Finally, Fig. 4 summarizes the solar-based experiments that took place in the PET Jerrycan, but in Lake Geneva water. The main difference is the change of matrix, hence the pathways under ques-

tion are the changes inflicted by the slightly higher pH (8.3 instead of 8.15), the ions (compared to tap water) and not the UV–vis transmittance of the material. SODIS took place effectively but was significantly delayed compared to the tap water experiments. In these experiments, a max. difference of 3 °C was observed, but since it is way below the germicidal threshold or the threshold to activate PMS (40 °C, (Rodríguez-Chueca et al., 2019)), we do not consider this as an influential factor. The main characteristic that differed among the experiments with tap water and lake water was the organic matter content. Although DOM has been long recognized as a source of bactericidal ROS and transient species (Kohantorabi et al., 2019; Vione et al., 2014), the dominant effect of its presence is the light filter (Ng et al., 2014). Most likely, the absence of the UVB irradiation due to the PET is of key influence for the generation of transient species (Serna-Galvis et al., 2018).

The hv/H_2O_2 process was severely hampered in lake water. Besides the already discussed loss of $HO^\bullet$ due to the lack of UVB irradiation, the small amount of $HO^\bullet$ generated is diminished by the inner filter effect of DOM, and the $HO^\bullet$ are most likely being scavenged by the DOM itself, as a target (Vione et al., 2006). The addition of Fe^{2+} has a detrimental effect on the efficacy on the process; although more UVA is available in PET, the lake water shows a higher absorbance after the addition of Fe, most likely via its complexation by DOM and the generation of photo-active complexes (Fig. S3). In some works, these complexes have been expected to contribute to maintaining the iron in solution and assist the photo-Fenton process (Giannakis et al., 2016; Porras et al., 2018; Rodríguez-Chueca et al., 2014), and indeed this may happen here in a small extent. Nevertheless, the possible higher $HO^\bullet$ generation is scavenged by DOM, as shown by the different spectra of tap and lake water (Fig. S3).

Surprisingly, the hv/PMS process was not as scavenged as the hv/H_2O_2 process. This means that the activation of PMS by light, although smaller (hence slower kinetics), continued to generate $HO^\bullet$ and $SO_4^{\bullet-}$. Considering that $SO_4^{\bullet-}$ reacts much more slowly with DOM compared to $HO^\bullet$, this explains why this process could maintain a high bactericidal efficacy. The addition of Fe^{2+} was once again found to be detrimental to the hv/PMS efficacy, but not high enough to hinder the solar-initiated pathways. Hence, the PMS-assisted processes are more effective than the respective H_2O_2 ones in natural waters; if one compares the kinetics of SODIS with the attained by the H_2O_2-based processes (231 and 141% increase) or with the PMS-based processes (715 and 538% increase), for the selected amounts of Fe, H_2O_2 and PMS, the importance of enhancing SODIS with either process (H_2O_2 or PMS-based) is more than obvious. What is more important, is that the PMS-based processes led to even higher enhancements, hence their superiority in PET reactors with natural waters is verified.

3.1.5. Significance of the disinfection findings

As a provisional conclusion, similarly to Keogh et al. and Garcia-Gil et al., (García-Gil et al., 2020a; Keogh et al., 2015) we can verify that both the 19-L PC water cooler bottles and the 25-L PET jerrycans are good candidates for SODIS containers, but also, our new results prove that they are suitable vectors for solar-based advanced oxidation processes, based on either $HO^\bullet$ and $SO_4^{\bullet-}$. The differences between material properties lead to changes in the pathways of bacterial inactivation, but both materials ensured total inactivation in less than 3–4 h (in any matrix), in compliance with the 1-day exposure necessities of SODIS, even at high volumes and at modest temperatures. Also, the addition of oxidants (H_2O_2, PMS) and Fe^{2+}, all enhanced SODIS; the studied oxidative processes were more effective than SODIS, hence the beneficial impact of $HO^\bullet$ and $SO_4^{\bullet-}$ cannot be doubted. Despite the generally unfavorable conditions, namely i) high pH in our matrices (alkaline pH), ii) the subsequent precipitation of iron and the possible deposition on the wall of the reactors, which may result in lower light penetration, iii) the passive, convectional mixing only due to temperature gradients, and iv) the heterogeneous catalytic pathways, the processes were found to be suitable and effective in reducing the bacterial load. However, before any conclusive recommendation can be made regarding the suitability of the process and the material selection, the effect of each process on the material must be assessed.

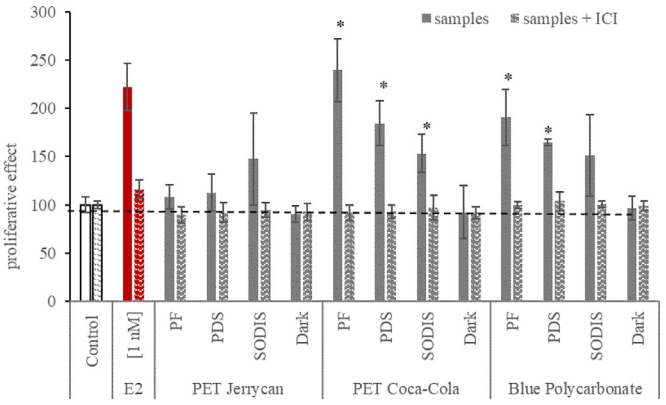

Fig. 5. Results of the E-screen assay in the presence and absence of ICI showing the proliferative effect of leachates from PET Jerrycan, PET Coca-Cola and blue polycarbonate following Photo-Fenton (PF), Peroxydisulfate activation (PDS) and Solar Disinfection (SODIS) irradiation treatments for 6 h.

3.2. Toxicity assays – Plastic leachables

3.2.1. Proliferative effects of leachables following 6 h of irradiation

The proliferative effects of migrating substances from PETjc, PETcc and blue PC plastic polymers following 6 h of irradiation with SODIS, photo-Fenton and persulfate activation (hv/PDS/Fe^{2+}) reactions are described in Fig. 5. In order to isolate the effects of plastic from other potential sources of contamination ultrapure MQ water was used and PDS as an exclusive sulfate radical generator was employed instead of PMS. The E-screen assay was carried out in the presence and absence of ICI 182,780, an estrogen receptor antagonist, to confirm whether any chemicals released under SODIS, photo-Fenton and PDS activation processes were estrogenic.

Following 6 h irradiation, no significant estrogenic activity was detected for PETjc pieces for any of the treatments (Fig. 5). Calculated relative proliferative effect (RPE) values of migrating substances from PETjc were around 5% for the photo-Fenton treatment, 7% for the PDS activation and 18% for SODIS (Table 4). These RPE values indicated that PETjc samples were very weak or non-existent agonists of estradiol and were therefore not estrogenic.

On the other hand, evidence of estrogenic activity was apparent in migrating substances from PETcc following 6 h irradiation. Relative to the negative control PETcc stimulated growth by 153 ± 20% following SODIS, 239 ± 32% following photo-Fenton conditions and by 184 ± 23% following a PDS activation process (Fig. 5). The data show an increase of approximately 31–86% in proliferation when SODIS irradiation treatment was enhanced. These proliferative effects translate to RPE of 76% for photo-Fenton treatment, 67% for PDS activation treatment and around 43% for SODIS (Table 4). These results suggest that substances released from PETcc act as partial agonists of the estradiol receptor.

Migrating substances from the PC bottle stimulated growth by 151 ± 42% following SODIS for 6 h (Fig. 5). However, this was not significantly different from the negative control. Substances released from PC after 6 h photo-Fenton and PDS activation reactions stimulated proliferation by 190 ± 29% and by 164 ± 4% respectively. The substances migrating from PC after 6 h of photo-Fenton

Table 4
Relative Proliferative Effects (RPE%) expressed as the mean ± standard deviation and Estradiol Equivalents (EEQ ng/L) of leachates from PET from a 25 L Jerrycan (PETjc), PET from a Coca-Cola bottle (PETcc) and the blue Polycarbonate bottle (PC) following various irradiation conditions. Green: non-estrogenic activity. Orange: weak/partially estrogenic. Red: estrogenic. Blue: safe for human consumption (according to (Kuch et al., 2010)). (For color refer to the online version.)

		PETjc		PETcc		PC	
Solar-based Treatments		RPE (%)	EEQ (ng/L)	RPE (%)	EEQ (ng/L)	RPE (%)	EEQ (ng/L)
1-day test	Photo-Fenton ($hv/H_2O_2/Fe^{2+}$)	4.87±7.10	8.40E-07	75.58±9.72	0.4	80.64±36.27	0.6
	PDS activation ($hv/PDS/Fe^{2+}$)	6.94±7.72	4.60E-06	67.13±20.78	0.2	49.23±14.91	0.1
	SODIS (*hv alone*)	17.72±22.06	4.10E-04	42.67±16.79	2.70E-02	43.52±27.08	3.00E-02
	Dark control	-	-	-	-	-	-
1-week test	Photo-Fenton ($hv/H_2O_2/Fe^{2+}$)	82.43±37.87	0.6	62.73±15.71	0.2	115.65±18.85	3.2
	PDS activation ($hv/PDS/Fe^{2+}$)	99.34±53.85	1.5	66.61±12.54	0.2	131.33±20.39	5.9
	SODIS (*hv alone*)	87.25±48.84	0.8	33.25±7.35	8.20E-03	95.95±25.54	1.3
	Dark control	12.72±12.98	8.30E-05	8.92±7.38	1.50E-05	17.96±12.30	4.30E-04

irradiation treatment had RPE of approximately 81% which implies that these released substances act as partial/total agonists of the estradiol receptor (Table 4). On the other hand, substances migrating from PC after 6 h of PDS activation triggered an RPE of 49% which suggests they are weak/partial agonists of the estradiol receptor (Table 4).

3.2.2. Proliferative effects of leachables following 7 days of irradiation

Evidence of time-dependent estrogenic activity of chemicals released from PETjc after 1 week of irradiation was shown. Relative to the negative control, PETjc leachates after 1 week of SODIS-stimulated growth by 210 ± 21%. Interestingly, no further increase in proliferation was observed when SODIS was enhanced. The substances released after 1 week under photo-Fenton irradiation and PDS activation stimulated proliferation by 216 ± 18% and by 244 ± 36%, respectively (Fig. 6). The RPE values of the leachates from PETjc polymer after 1 week under irradiation treatment were ≥ 80% which indicated a strong estradiol agonistic effect of the samples (Table 4). Also important to note here, is that prolonged irradiation of PETcc for a week did not significantly enhance estrogenic activity when compared to the levels of estrogenicity detected following 6 h irradiation of the samples. However, enhanced SODIS conditions with PETcc led to a 41–43%% increase in proliferation. Estrogenic activity of migrating chemicals from PETcc released after 1 week under SODIS, photo-Fenton and PDS activation conditions were 139 ± 7%, 180 ± 26% and 182 ± 23% respectively relative to the control (Fig. 6). RPE values between approximately 33–67% indicate that the leachates released from the PETcc after one week of irradiation treatment act as partial agonists of the estradiol receptor.

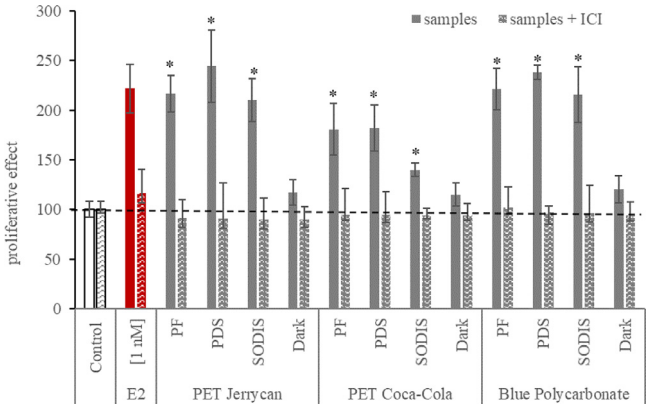

Fig. 6. Results of the E-screen assay in the presence and absence of ICI showing the proliferative effect of leachates from PET from a 25-L Jerrycan (PETjc), PET from a Coca-Cola bottle (PETcc) and the blue Polycarbonate bottle (PC), following Photo-Fenton (PF), Peroxydisulfate activation (PDS) and Solar Disinfection (SODIS) irradiation treatments for 1 week.

Evidence of time-dependent estrogenic activity was also apparent in PC leachables. Prolonged irradiation of PC over the course of 1 week enhanced estrogenic activity when compared to the estrogenic activity of the samples irradiated for 6 h. Estrogenic activity of released substances from blue PC under SODIS, photo Fenton and PDS activation were 216 ± 21%, 221 ± 21% and 238 ± 7% respectively relative to the control (Fig. 6). The RPE values of the PC irradiated for 1 week were ≥ 80% (Table 4), meaning that they are strong estradiol agonists. Moreover, PC leachates from advanced oxidative processes were above 100% indicating an estrogenic affect more potent than the one exerted by the positive control estradiol. Co-incubation of all leachates with ICI had a negligible effect on growth compared with the negative control confirming the presence of estrogenic leachables (see Fig. 6).

3.2.3. Estradiol equivalents (EEQs)

Estradiol equivalent values (EEQs) were calculated for all leachates that showed an increased proliferative effect to benchmark water in terms of acceptable daily intake limit of β-estradiol set by JECFA (2000) (Table 4). EEQ values calculated from the dose-response curve of 17β-estradiol were corrected for the concentration factor used. Since water samples were concentrated 10,000-fold via SPE and diluted 100-fold in the E-screen the final concentration factor for every sample was 100. Derived EEQs were reported as ng/L. The values calculated ranged from 0.008 – 5.9 ng/L.

Following 6 h irradiation, the EEQ values for the samples from the blue polycarbonate polymer (PC) were in the order of 0.03–0.57 ng/L and were the highest values obtained for all three plastics. EEQ values for the PETjc samples were 10^3 to 10^6 times lower than 1 ng/L while the EEQ values for PETcc samples were greater than the values for the PETjc and were in the order of 0.03–0.42 ng/L.

Following 1 week of irradiation, the EEQ values for the PC samples were in the order of 1.3–5.9 ng/L and were again the highest values obtained for all three plastics for that period of irradiation. EEQ values of the PETjc samples were in the order of 0.6–1.5 ng/L while the EEQ values for PETcc samples were in the order of 0.008–0.2 ng/L and unlike following 6 h of irradiation were lower than the values obtained for the PETjc.

Assuming a 3.5 kg baby consumes 0.52 L water through breast milk, the daily consumption of estradiol from the PDS-irradiated water (sample having the highest EEQ value) would be 0.9 ng/kg of body weight. The corresponding value for an adult of 65 kg that drinks 2 L of water per day would be 0.2 ng/kg of body weight. All values calculated were within the ADI range (0–50 ng/kg body weight) of estradiol recommended by the JECFA (World Health Organization, 2006).

3.2.4. Mutagenicity of leachables

No mutagenicity was detected for any sample when tested using the Ames test as no value obtained showed a clear fold induction ≥2 above the baseline value (Table 5).

3.2.5. Significance of the toxicological findings

Known substances and unknown NIAS can migrate from plastics in contact with water and so testing the overall migrate using in vitro tests offers a pragmatic and cost-effective approach to toxicity testing. In vitro toxicity testing performed with FCMs has focused on 3 main types of toxicity, namely cytotoxicity, genotoxicity, and endocrine activity (Groh and Muncke, 2017). In this study, genotoxicity was tested using the Ames test and endocrine activity was determined using the E-screen assay. The study by De Fusco et al. in 1990 was among the earliest investigations for the presence of toxins in bottled water (De Fusco et al., 1990). They studied the leaching of mutagens into mineral water from PET bottles using the Ames test following short and long-term storage in light and dark. The results identified leaching of mutagens after 1 month of storage but not after 3 or 6 months of storage. The mutagenic activity detected in the water stored for 1 month in PET was higher after storage in daylight compared with storage in the dark. Since then, a number of similar studies have been carried out (Bach et al., 2014, 2013; Monarca et al., 1994; Ubomba-Jaswa et al., 2010). As was the case in this study, no mutagenicity was reported in any of these studies, with the exception of that by Ubomba-Jaswa et al. (Ubomba-Jaswa et al., 2010). However, in their study, while genotoxicity was detected after 2 months in water stored in PET bottles and exposed continuously (without refilling) to sunlight, toxicity was also detected in PET bottles stored in the dark after 2 months making it unlikely that the genotoxicity was related to solar treatment.

A number of studies have suggested the presence of endocrine disruptors in PET-bottled water as well as most plastics using the E-screen including Wagner and Oehlmann (Wagner and Oehlmann, 2011) and Yang et al. (Yang et al., 2011). The E Screen bioassay, also known as the MCF-7 cell proliferation bioassay, was the first in vitro bioassay developed for screening estrogenic activity. It measures cellular estrogen-dependent proliferation of the MCF-7 human breast cancer cell line. While no mutagenicity was detected in this study, levels of estrogenicity were detected in some samples. In the case of the SODIS process, no significant levels of estrogenicity were detected for the PETjc plastic following 6 h irradiation. However, partial estrogenicity was detected for the PETcc and weak estrogenicity was detected for the PC plastic when tested for the same period of time. Differences in results obtained for different PET plastics has been attributed to different sources of manufacture for the plastic (Groh and Muncke, 2017). Another difference between the PET plastics used in this study was the age

Table 5
The results of the Ames test for leachables from PETjc (JC), PETcc (CC) and blue polycarbonate (PC) following 6 h and 1 week of different irradiation treatments. The test used the strains *S. typhimurium* TA98 and TAMix with (+) and without (-) S9. Results were reported as the mean of the fold induction over the baseline ± standard deviation.

Duration	Plastic Polymer	Irradiation Treatment	TA 98 (+S9)	TA 98 (-S9)	TA mix (+S9)	TA mix (-S9)
CONTROLS		Control	3.34±1.17	3.42±1.03	1.9 ± 0.7	2.78±1.3
		Positive control	41.53±1.93	45.87±2.59	23.06±1.16	40±2.87
1-day test	JC	Photo-Fenton ($hv/H_2O_2/Fe^{2+}$)	0.33±1.53	0.62±3.21	0.55±1.00	1.00±1.00
		PDS activation ($hv/PDS/Fe^{2+}$)	1.00±1.00	0.80±0.58	0.70±1.53	0.32±1.53
		SODIS (hv alone)	0.82±1.53	1.00±2.00	1.00±0.00	0.44±0.58
		Dark control	0.20±0.00	0.49±2.08	0.67±0.58	1.33±0.58
	CC	Photo-Fenton ($hv/H_2O_2/Fe^{2+}$)	1.00±1.00	0.44±0.58	0.55±1.00	0.67±0.58
		PDS activation ($hv/PDS/Fe^{2+}$)	1.67±1.15	0.69±1.73	0.52±0.00	0.56±1.53
		SODIS (hv alone)	0.23±0.58	0.17±0.58	0.12±0.58	0.56±1.15
		Dark control	0.60±1.00	0.14±1.15	0.33±0.58	0.67±2.31
	PC	Photo-Fenton ($hv/H_2O_2/Fe^{2+}$)	0.83±1.53	0.36±1.53	1.00±0.00	2.67±1.53
		PDS activation ($hv/PDS/Fe^{2+}$)	1.33±1.15	1.15±0.58	0.35±0.58	0.32±1.53
		SODIS (hv alone)	0.58±1.53	1.00±2.00	0.12±0.58	0.56±1.53
		Dark control	0.47±1.53	0.28±0.58	0.67±0.58	0.50±0.00
1-week test	JC	Photo-Fenton ($hv/H_2O_2/Fe^{2+}$)	0.50±2.00	0.80±3.00	0.55±1.00	1.33±0.58
		PDS activation ($hv/PDS/Fe^{2+}$)	1.50±1.00	0.46±0.58	0.35±0.58	0.24±1.00
		SODIS (hv alone)	0.82±1.53	0.17±0.58	1.00±0.00	0.67±1.00
		Dark control	0.53±0.58	0.42±1.73	0.17±0.58	0.83±0.58
	CC	Photo-Fenton ($hv/H_2O_2/Fe^{2+}$)	0.17±0.58	0.27±1.00	0.18±0.58	1.67±2.08
		PDS activation ($hv/PDS/Fe^{2+}$)	1.17±0.58	0.46±1.53	0.17±0.58	0.48±1.00
		SODIS (hv alone)	0.23±0.58	1.17±2.31	0.35±1.00	0.44±1.53
		Dark control	0.20±1.00	0.28±0.58	0.33±0.58	1.50±1.00
	PC	Photo-Fenton ($hv/H_2O_2/Fe^{2+}$)	0.33±0.58	0.27±1.00	0.37±0.58	2.33±1.15
		PDS activation ($hv/PDS/Fe^{2+}$)	1.33±2.08	0.69±2.00	0.17±0.58	0.40±0.58
		SODIS (hv alone)	0.35±1.00	1.33±0.58	0.47±0.58	0.33±1.00
		Dark control	0.40±0.00	0.35±0.58	0.33±1.15	1.50±0.00

of the plastic. While the PETjc plastic was new, the PETcc plastic while of food grade was not new. Andra et al. found that the greatest contributor to the release of chemicals from PET and PC was the number of times the container was used (Andra et al., 2011).

In recent times, interest has grown in using plastics other than PET in the SODIS process. Fisher et al., investigated the use of 1-L polycarbonate bottles (Fisher et al., 2012b), while Keogh et al. carried out comparative studies of the bacterial inactivation efficacy of 19 L polycarbonate water dispenser containers similar to that used in this study (Keogh et al., 2015). In their review, Borde et al. considered the challenges faced using large plastic bottles such as water dispensing containers made of polycarbonate in SODIS studies including the fear of leaching from the plastic container into the water (Borde et al., 2016). Bisphenol-A (BPA) is an additive used in the manufacture of PC and is a known weakly estrogenic endocrine disruptor. The PC container used in this study like the PETcc was also reused plastic and leaching of BPA from reusable PC drinking bottles has been previously reported (Kubwabo et al., 2009). Another distinguishing feature of the PC plastic was its blue color. Colorants are among the additives that can be used in plastic manufacture. In nearly all cases, additives are not chemically bound to the plastic polymer (Hahladakis et al., 2018), and so could be leached under abnormal conditions.

Furthermore, no significant estrogenicity was detected for the AOP processes carried out for 6 h in PETjc, however, increases in the levels of estrogenicity were detected for the AOPs for both the PETcc and the PC plastics. We are not aware of any toxicity studies on similar AOPs, however in their study on the effect of reactor material and its reuse on the photo-Fenton process, Varón-López et al. (López et al., 2017) found improved disinfection using photo-Fenton in reused PET reactors which they attributed to additional ROS produced by material degradation. They questioned the stability of PET after continuous exposure to a highly oxidative process such as photo-Fenton and suggested that toxicity testing be carried out on such systems to evaluate the safety of the water.

Concerning the disinfection methods used, the increase in estrogenicity was greater for the photo-Fenton process than for persulfate activation. This trend mirrored the bacterial disinfection kinetics obtained under similar environmental conditions of temperature and water composition suggesting that the $HO^{\bullet}$ radicals had a more pronounced affect on leaching than the $SO_4^{\bullet-}$ radicals. In our study, the levels of estrogenicity detected following 6 h incubation for PETcc and PC were significantly higher than those detected for PETjc. The amount of plastic used in the tests replicated the plastic to water ratio in the original vessel suggesting that the ratio of plastic to volume of water treated also plays a role.

When the time of solar treatment was extended beyond the normal exposure time to seven continuous days of irradiation all three plastics showed estrogenicity. The levels of estrogenicity detected were determined not to be a threat to human health. Nevertheless, these preliminary findings indicate the need for further toxicity studies of these AOPs. This study was designed to investigate a worst-case scenario by immersing pieces of plastic in the water. Future studies should investigate water samples taken from operating reactors and consider the effect of varying environmental conditions including the water matrix on toxicity. The study of mutagenicity and estrogenicity is very relevant when using plastic reactors for solar disinfection. However, detection of toxicity using these bioassays should be followed up with chemical analysis in order to identify the toxic substance and its concentration.

Recent long term (>12 months) field studies in Malawi of 20 L polypropylene transparent SODIS buckets (Morse et al., 2020; Polo-López et al., 2019) have shown that those portions of the SODIS container that remain out of contact with the water stored inside (e.g. near the upper rim), deteriorate at a faster rate than those portions of the container that remain in more sustained contact with the stored water (e.g. nearer the base of the bucket). The possibility that the risk posed from photo-degradation products varies with container geometry merits further study.

4. Conclusions

As the needs for higher quantities of safe water in rural and peri–urban communities in sunny and developing countries grows, the assessment of cheap large-scale reactors for SODIS implementation and its enhancement is a necessity. From the results of this work we can draw the following conclusions:

- SODIS took place effectively in both tested materials (PC or PET), and the real water matrices were completely disinfected (5-log units). This effect took place much earlier than the envisioned time of exposure to solar light in the field, despite the water matrix constituents, basic pH and organic matter presence, even in a more unfavorable geographic latitude (Switzerland) than the usual SODIS applications.
- Both enhancements (H_2O_2 and PMS, with or without Fe^{2+}) were highly effective and halved (or more) the necessary exposure time to achieve complete disinfection. Hence, the choice of the method would ultimately be affected by the reagent costs and availability in the region of application. Nevertheless, H_2O_2 and photo-Fenton are favored in PC bottles due to the UVB portion transmitted in the reactor and PMS-based enhancements thrived in PET reactors where visible light was transmitted in higher proportions.
- Since the temperature was kept low (<36 °C) in all tests, the necessity to increase the temperature in order to effectively eliminate bacterial pathogens by SODIS is now proven secondary. However, this has to be very cautiously generalized to other pathogens (e.g. viruses, Cryptosporidium), pending further testing.
- Generally, PC was found to leach slightly more estrogenic compounds than PET. Also, if we classify the disinfection methods in a tentative order of risk, we get SODIS<PDS<photo-Fenton, for short term testing and SODIS<pF<PDS after 1 week. The difference is attributed to the type and progression of the oxidative attacks by sulfate vs. hydroxyl radicals.
- Despite the apparent increase in estrogenic compounds, none of the materials and none of the processes led to the generation of dangerous amounts of leachables, when average daily drinking water intake was considered. In addition, no mutagenicity was noted. Although these constitute very encouraging results, further testing of materials and treatment methods should be considered. Also, if the water is destined for immediate consumption, besides the materials effect, the need to assess the residual effects of oxidants' addition should not be overlooked.

In conclusion, we propose that solar-based enhancements should be further assessed as improvements of drinking water quality, since bacteria can be eliminated, and oxidative processes such as photo-Fenton and persulfate are known to reduce natural organic matter loads. Although SODIS still remains the most cost-effective, simple, and reliable technology, their compatibility with methods providing larger than the typical 2-L SODIS volumes makes them a great ally in the supply of safe drinking water at larger or community level scale.

Declaration of Competing Interest

The authors declare that they have no known competing financial interests or personal relationships that could have appeared to influence the work reported in this paper.

Acknowledgements

The authors acknowledge the financial support of the European Union's Horizon 2020 research and innovation program in the frame of the WATERSPOUTT H2020-Water-5c-2015 project (H2020 GA 688928) project. Stefanos Giannakis would like to acknowledge the Spanish Ministry of Science, Innovation and Universities (MICIU) for the Ramón y Cajal Fellowship (RYC2018–024033-I). Rosaleen Devery would like to acknowledge Professor Ana M.Soto, Tufts University School of Medicine, Boston, MA02111 for kind donation of MCF-BOS cells. The authors would also like to acknowledge the contribution of Javier Marugán and Angela Garcia-Gil (URJC, Spain), and Inmaculada Polo-Lopez (CIEMAT-PSA, Spain) to providing details on the properties of the plastic materials. Also, the technical assistance of Dominique Grandjean and Florian Breider of GR-CEL (EPFL, Switzerland) for the SPE of the samples is greatly appreciated.

Supplementary materials

Supplementary material associated with this article can be found, in the online version, at doi:10.1016/j.watres.2020.116387.

References

Abbas, A., Schneider, I., Bollmann, A., Funke, J., Oehlmann, J., Prasse, C., Schulte-Oehlmann, U., Seitz, W., Ternes, T., Weber, M., Wesely, H., Wagner, M., 2019. What you extract is what you see: optimising the preparation of water and wastewater samples for in vitro bioassays. Water Res. 152, 47–60. https://doi.org/10.1016/J.WATRES.2018.12.049.

Andra, S.S., Makris, K.C., Shine, J.P., 2011. Frequency of use controls chemical leaching from drinking-water containers subject to disinfection. Water Res. 45, 6677–6687.

Baatout, S., De Boever, P., Mergeay, M., 2005. Temperature-induced changes in bacterial physiology as determined by flow cytometry. Ann. Microbiol. 55, 73–80.

Bach, C., Dauchy, X., Severin, I., Munoz, J.-.F., Etienne, S., Chagnon, M.-.C., 2014. Effect of sunlight exposure on the release of intentionally and/or non-intentionally added substances from polyethylene terephthalate (PET) bottles into water: chemical analysis and in vitro toxicity. Food Chem. 162, 63–71.

Bach, C., Dauchy, X., Severin, I., Munoz, J.-.F., Etienne, S., Chagnon, M.-.C., 2013. Effect of temperature on the release of intentionally and non-intentionally added substances from polyethylene terephthalate (PET) bottles into water: chemical analysis and potential toxicity. Food Chem. 139, 672–680.

Berney, M., Weilenmann, H.U., Simonetti, A., Egli, T., 2006. Efficacy of solar disinfection of Escherichia coli, Shigella flexneri, Salmonella Typhimurium and Vibrio cholerae. J. Appl. Microbiol. 101, 828–836. https://doi.org/10.1111/j.1365-2672.2006.02983.x.

Bichai, F., Polo-López, M.I., Fernández, Ibañez, Polo-Lopez, P., Fernandez Ibanez, M.I., 2012. Solar disinfection of wastewater to reduce contamination of lettuce crops by Escherichia coli in reclaimed water irrigation. Water Res. 46, 6040–6050. https://doi.org/10.1016/j.watres.2012.08.024.

Blaustein, R.A., Pachepsky, Y., Hill, R.L., Shelton, D.R., Whelan, G., 2013. Escherichia coli survival in waters: temperature dependence. Water Res. 47, 569–578. https://doi.org/10.1016/j.watres.2012.10.027.

Borde, P., Elmusharaf, K., McGuigan, K.G., Keogh, M.B., 2016. Community challenges when using large plastic bottles for Solar Energy Disinfection of Water (SODIS). BMC Public Health 16, 931.

Bosshard, F., Bucheli, M., Meur, Y., Egli, T., 2010a. The respiratory chain is the cell's Achilles' heel during UVA inactivation in Escherichia coli. Microbiology 156, 2006–2015.

Bosshard, F., Riedel, K., Schneider, T., Geiser, C., Bucheli, M., Egli, T., 2010b. Protein oxidation and aggregation in UVA-irradiated Escherichia coli cells as signs of accelerated cellular senescence. Env. Microbiol. 12, 2931–2945. https://doi.org/10.1111/j.1462-2920.2010.02268.x.

Byrne, J.A., Dunlop, P.S.M., Hamilton, J.W.J., Fernández-Ibáñez, P., Polo-López, I., Sharma, P.K., Vennard, A.S.M., 2015. A review of heterogeneous photocatalysis for water and surface disinfection. Molecules 20, 5574–5615.

Castro-Alférez, M., Polo-López, Inmaculada, M., Marugán, J., Fernández-Ibáñez, 2018. Validation of a solar-thermal water disinfection model for Escherichia coli inactivation in pilot scale solar reactors and real conditions. Chem. Eng. J. 331, 831–840. https://doi.org/10.1016/j.cej.2017.09.015.

Castro-Alférez, M., Polo-López, M.I., Fernández-Ibáñez, P., 2016. Intracellular mechanisms of solar water disinfection. Sci. Rep. 6, 38145.

Castro-Alférez, M., Polo-López, M.I., Marugán, J., Fernández-Ibáñez, P., 2017. Mechanistic modeling of UV and mild-heat synergistic effect on solar water disinfection. Chem. Eng. J. 316, 111–120.

De Fusco, R., Monarca, S., Biscardi, D., Pasquini, R., Fatigoni, C., 1990. Leaching of mutagens into mineral water from polyethyleneterephthalate bottles. Sci. Total Environ. 90, 241–248.

European Commission, 2011. Commission Regulation (EU) No 10/2011 of 14 January 2011 on plastic materials and articles intended to come into contact with food. Off J Eur Union 12, 1–89.

European Commission, 2004. Regulation (EC) No 1935/2004 of the European Parliament and of the Council of 27 October 2004 on materials and articles intended to come into contact with food and repealing Directives 80/590/EEC and 89/109/EEC. EEC.

Farinelli, G., Minella, M., Pazzi, M., Giannakis, S., Pulgarin, C., Vione, D., Tiraferri, A., 2020. Natural iron ligands promote a metal-based oxidation mechanism for the Fenton reaction in water environments. J. Hazard. Mater. 393, 122413. https://doi.org/10.1016/j.jhazmat.2020.122413.

Ferreira, L.C., Castro-Alférez, M., Nahim-Granados, S., Polo-López, M.I., Lucas, M.S., Puma, G., Li, Fernández-Ibáñez, P., 2020. Inactivation of water pathogens with solar photo-activated persulfate oxidation. Chem. Eng. J. 381. https://doi.org/10.1016/j.cej.2019.122275.

Fisher, M.B., Iriarte, M., Nelson, K.L., 2012a. Solar water disinfection (SODIS) of Escherichia coli, Enterococcus spp., and MS2 coliphage: effects of additives and alternative container materials. Water Res. 46, 1745–1754. https://doi.org/10.1016/j.watres.2011.12.048.

Fisher, M.B., Iriarte, M., Nelson, K.L., 2012b. Solar water disinfection (SODIS) of Escherichia coli, Enterococcus spp., and MS2 coliphage: effects of additives and alternative container materials. Water Res. 46, 1745–1754. https://doi.org/10.1016/j.watres.2011.12.048.

Flanagan, J., Griffith, W.P., Skapski, A.C., 1984. The active principle of Caro's acid, HSO 5–: x-ray crystal structure of KHSO 5• H 2 O. J. Chem. Soc. Chem. Commun. 1574–1575.

García-Gil, Á., Pablos, C., García-Muñoz, R.A., McGuigan, K.G., Marugán, J., 2020a. Material selection and prediction of solar irradiance in plastic devices for application of solar water disinfection (SODIS) to inactivate viruses, bacteria and protozoa. Sci. Total Environ. 730, 139126. https://doi.org/10.1016/j.scitotenv.2020.139126.

García-Gil, Á., Valverde, R., García-Muñoz, R.A., McGuigan, K.G., Marugán, J., 2020b. Solar Water Disinfection in high-volume containers: are naturally occurring substances attenuating factors of radiation? Chem. Eng. J., 125852. https://doi.org/10.1016/j.cej.2020.125852.

Giannakis, S., 2018. Analogies and differences among bacterial and viral disinfection by the photo-Fenton process at neutral pH: a mini review. Environ. Sci. Pollut. Res.. https://doi.org/10.1007/s11356-017-0926-x.

Giannakis, S., Darakas, E., Escalas-Cañellas, A., Pulgarin, C., 2014a. Elucidating bacterial regrowth: effect of disinfection conditions in dark storage of solar treated secondary effluent. J. Photochem. Photobiol. A Chem. 290. https://doi.org/10.1016/j.jphotochem.2014.05.016.

Giannakis, S., Darakas, E., Escalas-Cañellas, A., Pulgarin, C., 2014b. The antagonistic and synergistic effects of temperature during solar disinfection of synthetic secondary effluent. J. Photochem. Photobiol. A Chem. 280. https://doi.org/10.1016/j.jphotochem.2014.02.003.

Giannakis, S., López, M.I.P., Spuhler, D., Pérez, J.A.S., Ibáñez, P.F., Pulgarin, C., 2016a. Solar disinfection is an augmentable, in situ-generated photo-Fenton reaction-Part 2: a review of the applications for drinking water and wastewater disinfection. Appl. Catal. B Environ. 198. https://doi.org/10.1016/j.apcatb.2016.06.007.

Giannakis, S., Merino Gamo, A.I., Darakas, E., Escalas-Cañellas, A., Pulgarin, C., 2013. Impact of different light intermittence regimes on bacteria during simulated solar treatment of secondary effluent: implications of the inserted dark periods. Sol. Energy 98. https://doi.org/10.1016/j.solener.2013.10.022.

Giannakis, Stefanos, López, Polo, Spuhler, M.I., Sánchez Pérez, D., Fernández Ibáñez, J.A., Pulgarin C., P., 2016b. Solar disinfection is an augmentable, in situ-generated photo-Fenton reaction—Part 1: a review of the mechanisms and the fundamental aspects of the process. Appl. Catal. B Environ. 199, 199–223. https://doi.org/10.1016/j.apcatb.2016.06.009.

Giannakis, S., Voumard, M., Rtimi, S., Pulgarin, C., 2018. Bacterial disinfection by the photo-Fenton process: extracellular oxidation or intracellular photo-catalysis? Appl. Catal. B Environ. 227, 285–295. https://doi.org/10.1016/j.apcatb.2018.01.044.

Groh, K.J., Muncke, J., 2017. In vitro toxicity testing of food contact materials: state-of-the-art and future challenges. Compr. Rev. Food Sci. Food Saf. 16, 1123–1150.

Guerra-Rodríguez, S., Rodríguez, E., Singh, D.N., Rodríguez-Chueca, J., 2018. Assessment of sulfate radical-based advanced oxidation processes for water and wastewater treatment: a review. Water (Basel) 10, 1828.

Hahladakis, J.N., Velis, C.A., Weber, R., Iacovidou, E., Purnell, P., 2018. An overview of chemical additives present in plastics: migration, release, fate and environmental impact during their use, disposal and recycling. J. Hazard. Mater. 344, 179–199.

Hairden, V.P., Harris, J.O., 1953. The isoelectric point of bacterial cells. J Bacteriol. 65 (2), 198–202.

Halstead, F.D., Ahmed, Z., Bishop, J.R.B., Oppenheim, B.A., 2019. The potential of visible blue light (405 nm) as a novel decontamination strategy for carbapenemase-producing enterobacteriaceae (CPE). Antimicrob. Resist. Infect. Control 8, 14. https://doi.org/10.1186/s13756-019-0470-1.

Hasan, N., Kim, S., Kim, M.S., Nguyen, N.T.T., Lee, C., Kim, J., 2020. Visible light-induced activation of peroxymonosulfate in the presence of ferric ions for the degradation of organic pollutants. Sep. Purif. Technol. 240, 116620. https://doi.org/10.1016/j.seppur.2020.116620.

Hessling, M., Spellerberg, B., Hoenes, K., 2017. Photoinactivation of bacteria by endogenous photosensitizers and exposure to visible light of different wavelengths - A review on existing data. FEMS Microbiol. Lett. 364, 1–12. https://doi.org/10.1093/femsle/fnw270.

Hoerter, J.D., Arnold, A.A., Kuczynska, D.A., Shibuya, A., Ward, C.S., Sauer, M.G., Gizachew, A., Hotchkiss, T.M., Fleming, T.J., Johnson, S., 2005. Effects of sublethal UVA irradiation on activity levels of oxidative defense enzymes and protein oxidation in Escherichia coli. J. Photochem. Photobiol. B Biol. 81, 171–180. https://doi.org/10.1016/j.jphotobiol.2005.07.005.

Huang, W., Bianco, A., Brigante, M., Mailhot, G., 2018. UVA-UVB activation of hydrogen peroxide and persulfate for advanced oxidation processes: efficiency, mechanism and effect of various water constituents. J. Hazard Mater. 347, 279–287. https://doi.org/10.1016/j.jhazmat.2018.01.006.

Keogh, M.B., Castro-Alférez, M., Polo-López, M.I., Calderero, I.F., Al-Eryani, Y.A., Joseph-Titus, C., Sawant, B., Dhodapkar, R., Mathur, C., McGuigan, K.G., 2015. Capability of 19-L polycarbonate plastic water cooler containers for efficient solar water disinfection (SODIS): field case studies in India. Bahrain Spain. Sol. Energy 116, 1–11.

Kohantorabi, M., Giannakis, S., Gholami, M.R., Feng, L., Pulgarin, C., 2019. A systematic investigation on the bactericidal transient species generated by photosensitization of natural organic matter (NOM) during solar and photo-Fenton disinfection of surface waters. Appl. Catal. B Environ. 983–995. https://doi.org/10.1016/j.apcatb.2018.12.012.

Kubwabo, C., Kosarac, I., Stewart, B., Gauthier, B.R., Lalonde, K., Lalonde, P.J., 2009. Migration of bisphenol A from plastic baby bottles, baby bottle liners and reusable polycarbonate drinking bottles. Food Addit. Contam. 26, 928–937.

Kuch, B., Kern, F., Metzger, J.W., von der Trenck, K.T., 2010. Effect-related monitoring: estrogen-like substances in groundwater. Environ. Sci. Pollut. Res. 17, 250–260. https://doi.org/10.1007/s11356-009-0234-1.

Liu, J., Zhao, Z., Shao, P., Cui, F., 2015. Activation of peroxymonosulfate with magnetic Fe3O4–MnO2 core–shell nanocomposites for 4-chlorophenol degradation. Chem. Eng. J. 262, 854–861.

López, A.V., López, K.H., Giannakis, S., Benítez, N., 2017. Effect of reactor material and its reuse on photo-Fenton process efficiency at near-neutral pH: alterations in E. coli inactivation and resorcinol degradation kinetics in water.. J. Photochem. Photobiol. A Chem. 344, 228–237. https://doi.org/10.1016/j.jphotochem.2017.04.019.

Maclean, M., McKenzie, K., Anderson, J.G., Gettinby, G., MacGregor, S.J., 2014. 405nm light technology for the inactivation of pathogens and its potential role for environmental disinfection and infection control. J. Hosp. Infect. 88, 1–11.

Marjanovic, M., Giannakis, S., Grandjean, D., de Alencastro, L.F., Pulgarin, C., 2018. Effect of MM Fe addition, mild heat and solar UV on sulfate radical-mediated inactivation of bacteria, viruses, and micropollutant degradation in water. Water Res. 140, 220–231. https://doi.org/10.1016/j.watres.2018.04.054.

Martínez-García, A., Vincent, M., Rubiolo, V., Domingos, M., Canela, Cristina, M., Oller, I., Fernández-Ibáñez, P. Polo-López, M.I., 2020. Assessment of a pilot solar V-trough reactor for solar water disinfection. Chem. Eng. J., 125719. https://doi.org/10.1016/j.cej.2020.125719.

Matzek, L.W., Carter, K.E., 2016. Activated persulfate for organic chemical degradation: a review. Chemosphere 151, 178–188.

McGuigan, K.G., Conroy, R.M., Mosler, H.J., du Preez, M., Ubomba-Jaswa, E., Fernandez-Ibañez, P., Fernandez-Ibanez, P., 2012. Solar water disinfection (SODIS): a review from bench-top to roof-top. J. Hazard Mater. 235–236, 29–46. https://doi.org/10.1016/j.jhazmat.2012.07.053.

McGuigan, K.G., Joyce, T.M., Conroy, R.M., Gillespie, J.B., Elmore-Meegan, M., 1998. Solar disinfection of drinking water contained in transparent plastic bottles: characterizing the bacterial inactivation process. J Appl Microbiol 84, 1138–1148.

Monarca, S., De Fusco, R., Biscardi, D., De Feo, V., Pasquini, R., Fatigoni, C., Moretti, M., Zanardini, A., 1994. Studies of migration of potentially genotoxic compounds into water stored in PET bottles. Food Chem. Toxicol. 32, 783–788.

Moncayo-Lasso, A., Sanabria, J., Pulgarin, C., Benitez, N., Benítez, N., Benitez, N., 2009. Simultaneous E. coli inactivation and NOM degradation in river water via photo-Fenton process at natural pH in solar CPC reactor. a new way for enhancing solar disinfection of natural water. Chemosphere 77, 296–300. https://doi.org/10.1016/j.chemosphere.2009.07.007.

Morse, T., Luwe, K., Lungu, K., Chiwaula, L., Mulwafu, W., Buck, L., Harlow, R., Fagan, G.H., McGuigan, K., 2020. A Transdisciplinary Methodology for Introducing Solar Water disinfection to rural communities in Malawi—formative research findings. Integr. Environ. Assess. Manag..

Mosteo, R., Varon Lopez, A., Muzard, D., Benitez, N., Giannakis, S., Pulgarin, C., 2020. Visible light plays a significant role during bacterial inactivation by the photo-fenton process, even at sub-critical light intensities. Water Res. 174, 115636. https://doi.org/10.1016/j.watres.2020.115636.

Nalwanga, R., Quilty, B., Muyanja, C., Fernandez-Ibañez, P., McGuigan, K.G., 2014. Evaluation of solar disinfection of E. coli under Sub-Saharan field conditions using a 25L borosilicate glass batch reactor fitted with a compound parabolic collector.. Sol. Energy 100, 195–202. https://doi.org/10.1016/j.solener.2013.12.011.

Ndounla, J., Pulgarin, C., 2014. Evaluation of the efficiency of the photo Fenton disinfection of natural drinking water source during the rainy season in the Sahelian region. Sci. Total Environ. 493, 229–238. https://doi.org/10.1016/j.scitotenv.2014.05.139.

Ndounla, J., Spuhler, D., Kenfack, S., Wéthé, J., Pulgarin, C., 2013. Inactivation by solar photo-Fenton in pet bottles of wild enteric bacteria of natural well water: absence of re-growth after one week of subsequent storage. Appl. Catal. B Environ. 129, 309–317. https://doi.org/10.1016/j.apcatb.2012.09.016.

Nelson, K.L., Boehm, A.B., Davies-Colley, R.J., Dodd, M.C., Kohn, T., Linden, K.G., Liu, Y., Maraccini, P.A., McNeill, K., Mitch, W.A., 2018. Sunlight-mediated inactivation of health-relevant microorganisms in water: a review of mechanisms and modeling approaches. Environ. Sci. Process. Impacts 20, 1089–1122.

Ng, T.-W.W., Chow, A.T., Wong, P.-K.K., 2014. Dual roles of dissolved organic matter in photo-irradiated Fe(III)-contained waters. J. Photochem. Photobiol. A Chem. 290, 116–124. https://doi.org/10.1016/j.jphotochem.2014.06.011.

Ng, T.W., Zhang, L., Liu, J., Huang, G., Wang, W., Wong, P.K., 2016. Visible-light-driven photocatalytic inactivation of Escherichia coli by magnetic Fe2O3–AgBr. Water Res. 90, 111–118. https://doi.org/10.1016/j.watres.2015.12.022.

Oppezzo, O.J., 2012. Contribution of UVB radiation to bacterial inactivation by natural sunlight. J. Photochem. Photobiol. B 115, 58–62. https://doi.org/10.1016/j.jphotobiol.2012.06.011.

Papadimitriou, E., Lelkes, P.I., 1993. Measurement of cell numbers in microtiter culture plates using the fluorescent dye Hoechst 33258. J. Immunol. Methods 162, 41–45. https://doi.org/10.1016/0022-1759(93)90405-V.

Pfeifer, G.P., You, Y.-H., Besaratinia, A., 2005. Mutations induced by ultraviolet light. Mutat. Res. Mol. Mech. Mutagen. 571, 19–31. https://doi.org/10.1016/j.mrfmmm.2004.06.057.

Polo-López, M.I., Fernández-Ibáñez, P., Ubomba-Jaswa, E., Navntoft, C., García-Fernández, I., Dunlop, P.S.M., Schmid, M., Byrne, J.A., McGuigan, K.G., 2011. Elimination of water pathogens with solar radiation using an automated sequential batch CPC reactor. J Hazard Mater 196, 16–21. https://doi.org/10.1016/j.jhazmat.2011.08.052.

Polo-López, M.I., Martínez-García, A., Abeledo-Lameiro, M.J., H Gómez-Couso, H.E., Ares-Mazás, E., Reboredo-Fernández, A., Morse, T.D., Buck, L., Lungu, K., McGuigan, K.G., 2019. Microbiological evaluation of 5L-and 20L-transparent polypropylene buckets for solar water disinfection (SODIS). Molecules 24, 2193.

Polo-López, M.I., Nahim-Granados, S., Fernández-Ibáñez, P., 2018. Homogeneous Fenton and Photo-Fenton Disinfection of Surface and Groundwater,. In: Applications of Advanced Oxidation Processes (AOPs) in Drinking Water Treatment. Springer, pp. 155–177.

Porras, J., Giannakis, S., Torres-Palma, R.A., Fernandez, J.J., Bensimon, M., Pulgarin, C., 2018. Fe and Cu in humic acid extracts modify bacterial inactivation pathways during solar disinfection and photo-Fenton processes in water. Appl. Catal. B Environ. 235. https://doi.org/10.1016/j.apcatb.2018.04.062.

Pulgarin, A., Giannakis, S., Pulgarin, C., Ludwig, C., Refardt, D., 2020. A novel proposition for a citrate-modified photo-Fenton process against bacterial contamination of microalgae cultures. Appl. Catal. B Environ. 265, 118615. https://doi.org/10.1016/j.apcatb.2020.118615.

Reyneke, B., Ndlovu, T., Vincent, M.B., Martínez-García, A., Polo-López, M.I., Fernández-Ibáñez, P., Ferrero, G., Khan, S., McGuigan, K.G., Khan, W., 2020. Validation of large-volume batch solar reactors for the treatment of rainwater in field trials in sub-Saharan Africa. Sci. Total Environ. 717. https://doi.org/10.1016/j.scitotenv.2020.137223.

Rijnaarts, H.H.M., Norde, W., Lyklema, J., Zehnder, A.J.B., 1995. The isoelectric point of bacteria as an indicator for the presence of cell surface polymers that inhibit adhesion. Colloids Surf. B Biointerfaces 4, 191–197. https://doi.org/10.1016/0927-7765(94)01164-Z.

Rincón, A.-.G., Pulgarin, C., 2007. Absence of< i>E. coliregrowth after Fe< sup>3+</sup>and TiO< sub>2</sub>solar photoassisted disinfection of water in CPC solar photoreactor. Catal. Today 124, 204–214.

Rodríguez-Chueca, J., Giannakis, S., Marjanovic, M., Kohantorabi, M., Gholami, M.R., Grandjean, D., de Alencastro, L.F., Pulgarín, C., 2019. Solar-assisted bacterial disinfection and removal of contaminants of emerging concern by Fe2+-activated HSO5- vs. S2O82- in drinking water. Appl. Catal. B Environ. 248, 62–72. https://doi.org/10.1016/J.APCATB.2019.02.018.

Rodríguez-Chueca, J., Polo-López, M.I., Mosteo, R., Ormad, M.P., Fernández-Ibáñez, P., 2014. Disinfection of real and simulated urban wastewater effluents using a mild solar photo-Fenton. Appl. Catal. B Environ. 150–151, 619–629. https://doi.org/10.1016/j.apcatb.2013.12.027.

Rodríguez-Chueca, J., Silva, T., Fernandes, J.R., Lucas, M.S., Puma, G.L., Peres, J.A., Sampaio, A., 2017. Inactivation of pathogenic microorganisms in freshwater using HSO5−/UV-A LED and HSO5−/Mn+/UV-A LED oxidation processes. Water Res. 123, 113–123. https://doi.org/10.1016/j.watres.2017.06.021.

Rommozzi, E., Giannakis, S., Giovannetti, R., Vione, D., Pulgarin, C., 2020. Detrimental vs. beneficial influence of ions during solar (SODIS) and photo-Fenton disinfection of E. coli in water: (Bi)carbonate, chloride, nitrate and nitrite effects. Appl. Catal. B Environ 270, 118877. https://doi.org/10.1016/j.apcatb.2020.118877.

Rosado-Lausell, S.L., Wang, H., Gutierrez, L., Romero-Maraccini, O.C., Niu, X.Z., Gin, K.Y., Croue, J.P., Nguyen, T.H., 2013. Roles of singlet oxygen and triplet excited state of dissolved organic matter formed by different organic matters in bacteriophage MS2 inactivation. Water Res. 47, 4869–4879. https://doi.org/10.1016/j.watres.2013.05.018.

Serna-Galvis, E.A., Troyon, J.A., Giannakis, S., Torres-Palma, R.A., Minero, C., Vione, D., Pulgarin, C., 2018. Photoinduced disinfection in sunlit natural waters: measurement of the second order inactivation rate constants between E. coli and photogenerated transient species.. Water Res. 147, 242–253. https://doi.org/10.1016/j.watres.2018.10.011.

Shekoohiyan, S., Rtimi, S., Moussavi, G., Giannakis, S., Pulgarin, C., 2019a. Enhancing solar disinfection of water in PET bottles by optimized in-situ formation of iron oxide films. From heterogeneous to homogeneous action modes with H_2O_2 vs. O_2 – Part 2: direct use of (natural) iron oxides. Chem. Eng. J. 360, 1051–1062. https://doi.org/10.1016/j.cej.2018.10.113.

Shekoohiyan, S., Rtimi, S., Moussavi, G., Giannakis, S., Pulgarin, C., 2019b. Enhancing solar disinfection of water in PET bottles by optimized in-situ formation of iron oxide films. From heterogeneous to homogeneous action modes with H_2O_2 vs. O_2 – Part 1: iron salts as oxide precursors. Chem. Eng. J. 358, 211–224. https://doi.org/10.1016/j.cej.2018.09.219.

Sinton, L.W., Finlay, R.K., Lynch, P.A., 1999. Sunlight inactivation of fecal bacteriophages and bacteria in sewage-polluted seawater. Appl. Environ. Microbiol. 65, 3605–3613.

Soto, A.M., Sonnenschein, C., Chung, K.L., Fernandez, M.F., Olea, N., Serrano3, F.O., Serrano, F.O., Serrano3, F.O., 1995. The E-SCREEN Assay as a Tool to Identify Estrogens: an Update on Estrogenic Environmental Pollutants. Environ. Health Perspect. 103, 113–122.

Spuhler, D., Rengifo-Herrera, J.A., Pulgarin, C., 2010. The effect of Fe2+, Fe3+, H202 and the photo-Fenton reagent at near neutral pH on the solar disinfection (SODIS) at low temperatures of water containing Escherichia coli K12. Appl. Catal. B. 96, 126–141. https://doi.org/10.1016/j.apcatb.2010.02.010.

Ubomba-Jaswa, E., Fernández-Ibáñez, P., McGuigan, K.G., 2010. A preliminary Ames fluctuation assay assessment of the genotoxicity of drinking water that has been solar disinfected in polyethylene terephthalate (PET) bottles. J. Water Health 8, 712–719. https://doi.org/10.2166/wh.2010.136.

Ubomba-Jaswa, E., Fernández-Ibáñez, P., Navntoft, C., Polo-López, M.I., McGuigan, K.G., 2010. Investigating the microbial inactivation efficiency of a 25L batch solar disinfection (SODIS) reactor enhanced with a compound parabolic collector (CPC) for household use. J. Chem. Technol. Biotechnol. 85, 1028–1037.

Vélez-Colmenares, J.J., Acevedo, A., Salcedo, I., Nebot, E., 2012. New kinetic model for predicting the photoreactivation of bacteria with sunlight. J. Photochem. Photobiol. B Biol. 117, 278–285. https://doi.org/10.1016//j.jphotobiol.2012.09.005.

Vione, D., Bagnus, D., Maurino, V., Minero, C., 2010. Quantification of singlet oxygen and hydroxyl radicals upon UV irradiation of surface water. Environ. Chem. Lett. 8, 193–198. https://doi.org/10.1007/s10311-009-0208-z.

Vione, D., Falletti, G., Maurino, V., Minero, C., Pelizzetti, E., Malandrino, M., Ajassa, R., Olariu, R.-I.I., Arsene, C., 2006. Sources and sinks of hydroxyl radicals upon irradiation of natural water samples. Environ. Sci. Technol. 40, 3775. https://doi.org/10.1021/es052206b.

Vione, D., Minella, M., Maurino, V., Minero, C., 2014. Indirect Photochemistry in Sunlit Surface Waters: photoinduced Production of Reactive Transient Species. Chem. – A Eur. J. 20, 10590–10606. https://doi.org/10.1002/chem.201400413.

Voelker, B.M., Morel, F.M.M., Sulzberger, B., 1997. Iron redox cycling in surface waters: effects of humic substances and light. Environ. Sci. Technol. 31, 1004–1011. https://doi.org/10.1021/es9604018.

Wagner, M., Oehlmann, J., 2011. Endocrine disruptors in bottled mineral water: estrogenic activity in the E-Screen. J. Steroid Biochem. Mol. Biol. 127, 128–135.

Wang, L., Zhang, Q., Chen, B., Bu, Y., Chen, Y., Ma, J., Rosario-Ortiz, F.L., Zhu, R., 2020. Some issues limiting photo(cata)lysis application in water pollutant control: a critical review from chemistry perspectives. Water Res. 174, 115605. https://doi.org/10.1016/j.watres.2020.115605.

Wegelin, M., Canonica, S., Alder, C., Marazuela, D., Suter, M.J.-F., Bucheli, T.D., Haefliger, O.P., Zenobi, R., McGuigan, K.G., Kelly, M.T., Ibrahim, P., Larroque, M., 2001. Does sunlight change the material and content of polyethylene terephthalate (PET) bottles? J. Water Supply Res. Technol. 50, 125–135. https://doi.org/10.2166/aqua.2001.0012.

Wegelin, M., Canonica, S., Mechsner, K., Fleischmann, T., Pesaro, F., Metzler, A., 1994. Solar water disinfection: scope of the process and analysis of radiation experiments. Aqua 43, 154–169.

World Health Organization, 2006. Toxicological Evaluation of Certain Veterinary Drug Residues in Food. World Health Organization.

Xiao, R., Bai, L., Liu, K., Shi, Y., Minakata, D., Huang, C.-H., Spinney, R., Seth, R., Dionysiou, D.D., Wei, Z., Sun, P., 2020. Elucidating sulfate radical-mediated disinfection profiles and mechanisms of Escherichia coli and Enterococcus faecalis in municipal wastewater. Water Res. 173. https://doi.org/10.1016/j.watres.2020.115552.

Xiao, R., Liu, K., Bai, L., Minakata, D., Seo, Y., Göktaş, R.K., Dionysiou, D.D., Tang, C.-J., Wei, Z., Spinney, R., 2019. Inactivation of pathogenic microorganisms by sulfate radical: present and future. Chem. Eng. J..

Yang, C.Z., Yaniger, S.I., Jordan, Vc.C., Klein, D.J., Bittner, G.D., 2011. Most plastic products release estrogenic chemicals: a potential health problem that can be solved. Environ. Health Perspect. 119, 989–996. https://doi.org/10.1289/ehp.1003220.

Zuo, Y., Hoigne, J., 1992. Formation of hydrogen peroxide and depletion of oxalic acid in atmospheric water by photolysis of iron (III)-oxalato complexes. Environ. Sci. Technol. 26, 1014–1022.